

Layer Adaptive Node Selection in Bayesian Neural Networks: Statistical Guarantees and Implementation Details

Sanket Jantre¹, Shrijita Bhattacharya^{*1}, and Tapabrata Maiti¹

¹Department of Statistics and Probability, Michigan State University

Abstract

Sparse deep neural networks have proven to be efficient for predictive model building in large-scale studies. Although several works have studied theoretical and numerical properties of sparse neural architectures, they have primarily focused on the edge selection. Sparsity through edge selection might be intuitively appealing; however, it does not necessarily reduce the structural complexity of a network. Instead pruning excessive nodes in each layer leads to a structurally sparse network which would have lower computational complexity and memory footprint. We propose a Bayesian sparse solution using spike-and-slab Gaussian priors to allow for node selection during training. The use of spike-and-slab prior alleviates the need of an ad-hoc thresholding rule for pruning redundant nodes from a network. In addition, we adopt a variational Bayes approach to circumvent the computational challenges of traditional Markov Chain Monte Carlo (MCMC) implementation. In the context of node selection, we establish the fundamental result of variational posterior consistency together with the characterization of prior parameters. In contrast to the previous works, our theoretical development relaxes the assumptions of the equal number of nodes and uniform bounds on all network weights, thereby accommodating sparse networks with layer-dependent node structures or coefficient bounds. With a layer-wise characterization of prior inclusion probabilities, we also discuss optimal contraction rates of the variational posterior. Finally, we provide empirical evidence to substantiate that our theoretical work facilitates layer-wise optimal node recovery together with competitive predictive performance.

Keywords: Node Selection, Dynamic Pruning, Model Compression, Spike-and-Slab Priors, Prior Inclusion Probability, Variational Inference, Contraction Rates

1 Introduction

Deep learning profoundly impacts science and society due to its impressive empirical success driven primarily by copious amounts of datasets, ever increasing computational resources, and deep neural network's (DNN) ability to learn task-specific representations. The key characteristic of deep learning is that accuracy empirically scales with the size of the model and the amount of training data. As such, large neural network models such as OpenAI GPT-3 (175 Billion) now typify the state-of-the-art across multiple domains such as natural language processing, computer vision, speech recognition etc. Nevertheless deep neural networks do have some drawbacks despite their wide ranging applications. First, this form of model scaling is exorbitantly prohibitive in terms of computational requirements, financial commitment, energy requirements etc. Second,

*corresponding author

DNNs tend to overfit leading to poor generalization in practice (Zhang et al., 2017). Finally, there are numerous scenarios where training and deploying such huge models is practically infeasible. Examples of such scenarios include federated learning, autonomous vehicles, robotics, recommendation systems where models have to be refreshed daily/hourly or in an online manner for optimal performance.

A promising direction for addressing these issues while improving the efficiency of DNNs is exploiting sparsity. From a practical perspective, it has been well-known that neural networks can be sparsified without significant loss in performance, Mozer and Smolensky (1988), and there is growing evidence that it is more so in the case of modern DNNs. Sparsity can arise naturally or be induced in multiple forms in DNNs, including input data, weights, and nodes. Weight pruning approaches often result in non-structured sparse deep neural architectures (Han et al., 2016; Molchanov et al., 2017; Zhu and Gupta, 2018; Frankle and Carbin, 2019). This might lead to inefficient computational gains in practical setups (Wen et al., 2016). Instead, inducing group sparsity on collection of incoming weights into a given node would reduce dimension of weight matrices per layer allowing for significant computational savings. Node selection in deep neural networks has been explored under frequentist setting in Alvarez and Salzmann (2016), Wen et al. (2016), and Scardapane et al. (2017) using group sparsity regularizers. On the other hand, Louizos et al. (2017), Neklyudov et al. (2017), and Ghosh et al. (2019) incorporate group sparsity via shrinkage priors in Bayesian paradigm. These group sparsity approaches specifically applied for node selection have shown significant computational speedup and lower memory footprint at inference stage in these preceding works. However, all of the proposed methods for sparsifying the neural networks perform ad-hoc pruning requiring fine-tuned thresholding rules. Our work alleviates the need of an ad-hoc thresholding rule for node selection through the use of spike-and-slab prior.

One of the major challenges in the implementation of sparse deep Bayesian neural networks (BNN) is computational complexity of the standard MCMC implementation. In the context of edge selection, variational inference as an alternative to MCMC (Jordan et al., 1999; Blei et al., 2017), has been explored both theoretically and numerically in the works of Blundell et al. (2015), Chérif-Abdellatif (2020), Bai et al. (2020). In the context of node selection, variational inference has been explored in the works of Louizos et al. (2017), Ghosh et al. (2019), etc. We improve upon existing literature in Bayesian node selection by using Gaussian spike and slab prior to allow for the exact setting of nodes to zero instead of ad-hoc pruning rules. Secondly, for scalability, we develop the variational Bayes solution to this problem and demonstrate its numerical performance in context of simulation and real data sets. Finally, we provide the theoretical guarantees to node selection under the most generalized scenario where the number of nodes in the model may vary as a function of the layer index. The development in this paper opens up the avenue to establish theoretical foundations of other variational inference based structured sparsity techniques, a problem which has not yet been explored in the literature.

Related Work: In the context of Bayesian neural networks, sparse DNNs have been studied in the works of Polson and Ročková (2018) and Sun et al. (2021). In the context of variational inference, sparse DNNs have been studied in the recent works of Chérif-Abdellatif (2020) and Bai et al. (2020). All these works concentrate on the problem of edge selection facilitated through the use of spike-and-slab priors with Gaussian slab distribution. In the context of node selection, Ghosh et al. (2019) makes use of regularized horseshoe prior. The main limitations of their approach include (1) need for fine tuning of the thresholding rule for node selection, and (2) lack of a theoretical justification.

The only two works which have provided theoretical guarantees of their proposed sparse DNN methods under variational inference include those of Chérif-Abdellatif (2020) and Bai et al. (2020). Since they focus on the problem of edge selection, their theoretical developments are related to the results of Schmidt-Hieber (2020) (see the sieve construction in relation (4) in Schmidt-Hieber (2020)). Thereby, they need certain restrictions on the network topology. Firstly, they assume equal number of nodes in each layer, secondly, they assume a known uniform bound B on all network weights and lastly, they assume a global sparsity parameter which may not lead to a structurally compact network. Although from a numerical standpoint, it may be

possible to extend the problem of edge selection implicitly to node selection, the theoretical extension to guarantee the node selection in sparse neural network is not immediate.

Detailed Contributions. In this paper, we assume a spike-and-slab prior where the slab provides control on the magnitude of incoming weights into a node and spike allows for the exact setting of nodes to 0.

For computational efficiency, we use a variational Bayes approach and establish its contraction rates in the context of node selection. In contrast to the existing works in the literature, we relax the assumption of equal number of nodes in each layer of the model. This

allows for the generalization of the theoretical development presented to guarantee the consistency of any generic shaped network structure. Contrary to the previous works, we relax the assumption of a uniform bound on all the coefficients of the neural network weights. Instead, we show that the slab part can provide a control on the growing weights in a given neural network architecture. We also derive explicit conditions on the prior parameters as a function of the layer to allow for the recovery of neural networks whose number of nodes and L_1 norm of incoming weights incident onto a node vary as a function of the layer index.

The notion of posterior contraction established in this work is in line of those established in Chérif-Abdellatif (2020) and Bai et al. (2020) but extended to the problem of node selection. In contrast to edge selection which controls the overall sparsity of the network, node selection provides structured sparsity through direct control on the number of neurons in each layer. We indeed show that the variational posterior based only on node selection can consistently recover the true function. There are two main advantages to node selection approach over edge selection (1) it has fewer parameters to train during optimization step (2) gives a compact network at inference step by setting several unimportant neurons to 0. In this work, we show that the contraction rates for the variational posterior varies as a function of the layer-wise node distribution in the sparse network and closeness of the true function to the space induced by the layer-wise node distribution. This theoretical development guides the calculation of layer-wise prior inclusion probabilities which allows for layer dependent node recovery in the computational experiments. Our numerical results validate the proposed theoretical framework for our neuron selection in DNN models. Further the proposed method achieves significant compression of DNN approximation in simulated as well as real datasets for classification and regression tasks. These empirical experiments further justify the use of layer-wise node inclusion probabilities to facilitate the optimal node recovery.

2 Nonparametric regression: deep learning approach

Consider the nonparametric regression model with p dimensional covariate \mathbf{X} .

$$Y_i = \eta_0(\mathbf{X}_i) + e_i, \quad i = 1, \dots, n, \quad (1)$$

where $e_i \stackrel{\text{i.i.d.}}{\sim} N(0, \sigma_e^2)$ (here i.i.d. denotes independent and identically distributed) and $\eta_0(\cdot) : \mathbb{R}^p \rightarrow \mathbb{R}$.

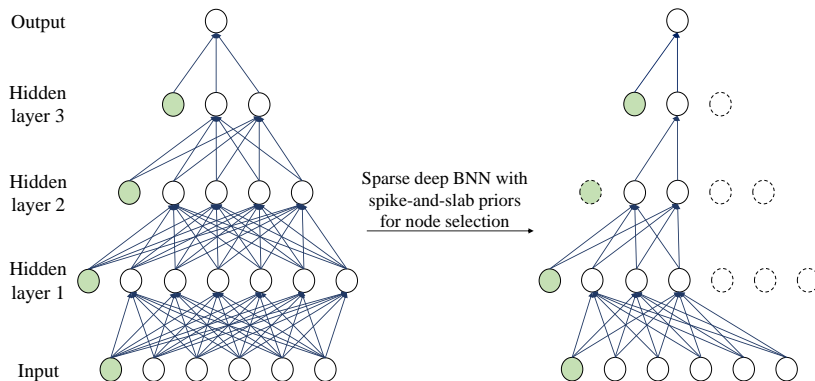


Figure 1: Sparse deep BNN using spike-and-slab priors achieves node selection in the given dense network on left leading to a sparse network on right.

Thus, the conditional distribution of $Y|\mathbf{X} = \mathbf{x}$ under the true model is

$$f_0(y|\mathbf{x}) = (\sqrt{2\pi\sigma_e^2})^{-1} \exp(-(y - \eta_0(\mathbf{x}))^2/(2\sigma_e^2)) \quad (2)$$

where \mathbf{x} is a feature vector from a marginal distribution $P_{\mathbf{X}}$ and y is the corresponding output from the conditional distribution $Y|\mathbf{X} = \mathbf{x}$.

Let $g: \mathbb{R}^p \rightarrow \mathbb{R}$ be a measurable function, then for some loss function \mathcal{L} , the risk of g is

$$R(g) = \int_{\mathcal{Y} \times \mathcal{X}} \mathcal{L}(Y, g(\mathbf{X})) dP_{\mathbf{X}, Y}$$

where $P_{\mathbf{X}, Y}$, the joint distribution of (\mathbf{X}, Y) is product of $P_{\mathbf{X}}$ and the conditional distribution $Y|X = \mathbf{x}$. (see Cannings and Samworth (2017) for more details). For the squared error loss, the above risk is minimized by $g^*(\mathbf{x}) = \eta_0(\mathbf{x})$ ((Friedman et al., 2009)). In practice, this estimator is not useful since $\eta_0(\mathbf{x})$ is unknown. Thus, an estimator of $\eta_0(\mathbf{x})$ is obtained based on the training observations, $\mathcal{D} = \{(\mathbf{x}_1, y_1), \dots, (\mathbf{x}_n, y_n)\}$, drawn from $P_{\mathbf{X}, Y}$. To find the class of optimal estimators, we use DNNs as an approximation to $\eta_0(\mathbf{x})$.

For a $p \times 1$ input vector \mathbf{x} , consider a DNN with L hidden layers with k_1, \dots, k_L as the number of nodes in the hidden layers denoted by $\eta_{\theta}(\mathbf{x})$. Also, $k_0 = p$ and $k_{L+1} = 1$. With $\overline{\mathbf{W}}_l = (\mathbf{v}_l, \mathbf{W}_l)$, we define

$$\eta_{\theta}(\mathbf{x}) = \mathbf{v}_L + \mathbf{W}_L \psi(\mathbf{v}_{L-1} + \mathbf{W}_{L-1} \psi(\dots \psi(\mathbf{v}_1 + \mathbf{W}_1 \psi(\mathbf{v}_0 + \mathbf{W}_0 \mathbf{x}))) \quad (3)$$

where \mathbf{v}_l and \mathbf{W}_l , $l = 0, \dots, L$ are $k_{l+1} \times 1$ vectors and $k_{l+1} \times k_l$ matrices, respectively and ψ is the activation function. Let $\theta = \{\overline{\mathbf{W}}_0, \dots, \overline{\mathbf{W}}_L\}$ denote all the parameters in the DNN model under consideration. Using the DNN in (3) to approximate the true function $\eta_0(\mathbf{x})$, the conditional distribution of $Y|\mathbf{X} = \mathbf{x}$ is

$$f_{\theta}(y|\mathbf{x}) = (\sqrt{2\pi\sigma_e^2})^{-1} \exp(-(y - \eta_{\theta}(\mathbf{x}))^2/(2\sigma_e^2))$$

Thus, the likelihood function for the data \mathcal{D} under the model and the truth is

$$P_{\theta}^n = \prod_{i=1}^n f_{\theta}(y_i|\mathbf{x}_i), \quad P_0^n = \prod_{i=1}^n f_0(y_i|\mathbf{x}_i). \quad (4)$$

For theoretical development in the subsequent sections we shall assume $P_{\mathbf{X}} = U[0, 1]^p$ and $\sigma_e^2 = 1$ and ψ is any 1-Lipschitz continuous activation function.

3 Node selection with spike-and-slab prior

To allow for automatic node selection, we consider a spike-and-slab prior consisting of a Dirac spike (δ_0) at 0 and a slab distribution (Mitchell and Beauchamp, 1988). The spike part is represented by an indicator variable which is set to 0 if a node is not present in the network. The slab part comes from a Gaussian distributed random variable. To allow for the layer-wise node selection, we assume that the prior inclusion probability λ_l varies as a function of the layer index l . The symbol i.d. is used to denote independently distributed random variables.

Prior: We assume a spike-and-slab prior of the following form with z_{lj} as the indicator for the presence of j^{th} node in the l^{th} layer

$$\overline{\mathbf{w}}_{lj}|z_{lj} \stackrel{\text{i.d.}}{\sim} [(1 - z_{lj})\delta_0 + z_{lj}N(0, \sigma_0^2\mathbf{I})], \quad z_{lj} \stackrel{\text{i.d.}}{\sim} \text{Ber}(\lambda_l)$$

where $l = 0, \dots, L$, $j = 1, \dots, k_{l+1}$. Also, $\overline{\mathbf{w}}_{lj} = (\overline{w}_{lj1}, \dots, \overline{w}_{lj k_{l+1}})$ is a vector of edges incident on the j^{th}

node in the l^{th} layer. In the above formula, note δ_0 is a Dirac spike vector of dimension $k_l + 1$ with all entries zero and \mathbf{I} is the identity matrix of dimension $k_l + 1 \times k_l + 1$. Furthermore, z_{lj} with $j = (1, \dots, k_{l+1})$ all follow Bernoulli(λ_l) to allow for common prior inclusion probability, λ_l , for each node from a given layer l . We set $\lambda_L = 1$ to ensure no node selection occurs in the output layer.

Posterior: With $\mathbf{z}_l = (z_{l1}, \dots, z_{lk_{l+1}})$, let $\mathbf{z} = (\mathbf{z}_1, \dots, \mathbf{z}_L)$ denote the vector of all indicator variables. The posterior distribution of $(\boldsymbol{\theta}, \mathbf{z})$ given \mathcal{D} is given by

$$\pi(\boldsymbol{\theta}, \mathbf{z}|\mathcal{D}) = \frac{P_{\boldsymbol{\theta}}^n \pi(\boldsymbol{\theta}|\mathbf{z}) \pi(\mathbf{z})}{\sum_{\mathbf{z}} \int P_{\boldsymbol{\theta}}^n \pi(\boldsymbol{\theta}|\mathbf{z}) \pi(\mathbf{z}) d\boldsymbol{\theta}} = \frac{P_{\boldsymbol{\theta}}^n \pi(\boldsymbol{\theta}|\mathbf{z}) \pi(\mathbf{z})}{m(\mathcal{D})} \quad (5)$$

where $P_{\boldsymbol{\theta}}^n = \prod_{i=1}^n f_{\boldsymbol{\theta}}(y_i|\mathbf{x}_i)$ is the likelihood function as in (4), $\pi(\mathbf{z})$ is the probability mass function of \mathbf{z} with respect to the counting measure and $\pi(\boldsymbol{\theta}|\mathbf{z})$ is the conditional probability density function with respect to the Lebesgue measure of $\boldsymbol{\theta}$ given \mathbf{z} . Further, $m(\mathcal{D})$ is the marginal density of the data and is free of $(\boldsymbol{\theta}, \mathbf{z})$.

Let $\tilde{\pi}(\boldsymbol{\theta}) = \sum_{\mathbf{z}} \pi(\boldsymbol{\theta}, \mathbf{z})$ be the marginal prior of $\boldsymbol{\theta}$. We shall use the notation

$$\tilde{\Pi}(\mathcal{A}) = \int_{\mathcal{A}} \tilde{\pi}(\boldsymbol{\theta}) d\boldsymbol{\theta} \quad (6)$$

to denote the probability distribution function corresponding to the density function $\tilde{\pi}$. The marginal posterior of $\boldsymbol{\theta}$ expressed as a function of the marginal prior for $\boldsymbol{\theta}$ is

$$\tilde{\pi}(\boldsymbol{\theta}|\mathcal{D}) = \sum_{\mathbf{z}} \pi(\boldsymbol{\theta}, \mathbf{z}|\mathcal{D}) = \frac{P_{\boldsymbol{\theta}}^n \tilde{\pi}(\boldsymbol{\theta})}{\int P_{\boldsymbol{\theta}}^n \tilde{\pi}(\boldsymbol{\theta}) d\boldsymbol{\theta}} = \frac{P_{\boldsymbol{\theta}}^n \tilde{\pi}(\boldsymbol{\theta})}{m(\mathcal{D})}$$

Thus, the probability distribution function corresponding to the density function $\tilde{\pi}(|\mathcal{D})$ is then given by

$$\tilde{\Pi}(\mathcal{A}|\mathcal{D}) = \int_{\mathcal{A}} \tilde{\pi}(\boldsymbol{\theta}|\mathcal{D}) d\boldsymbol{\theta} \quad (7)$$

Variational family: We posit the following mean field variational family (\mathcal{Q}^{MF}) on network weights as

$$\mathcal{Q}^{\text{MF}} = \left\{ \bar{w}_{lj} | z_{lj} \stackrel{\text{i.d.}}{\sim} [(1 - z_{lj})\delta_0 + z_{lj}N(\boldsymbol{\mu}_{lj}, \text{diag}(\boldsymbol{\sigma}_{lj}^2))], \quad z_{lj} \stackrel{\text{i.d.}}{\sim} \text{Ber}(\gamma_{lj}) \right\}$$

for $l = 0, \dots, L$, $j = 1, \dots, k_{l+1}$. This ensures that weight distributions follow spike-and-slab structure which allows for node sparsity through variational approximation. Further, the weight distributions conditioned on the node indicator variables are all independent of each other (hence use of the term mean field family). The variational distribution of parameters obtained post optimization will then inherently prune away redundant nodes from each layer. Also, Gaussian distribution for slab component is widely popular for approximating neural network weight distributions (Blundell et al., 2015; Louizos et al., 2017; Bai et al., 2020).

Additionally, $\boldsymbol{\mu}_{lj} = (\mu_{lj1}, \dots, \mu_{lj k_{l+1}})$ and $\boldsymbol{\sigma}_{lj}^2 = (\sigma_{lj1}^2, \dots, \sigma_{lj k_{l+1}}^2)$ denote the vectors of variational mean and standard deviation parameters of the edges incident on the j^{th} node in the l^{th} layer. Similarly, γ_{lj} denotes the variational inclusion probability of the j^{th} node in the l^{th} layer. We set $\gamma_{Lj} = 1$ to ensure no node selection occurs in the output layer.

Variational posterior: Variational posterior aims to reduce the Kullback-Leibler (KL) distance between a variational family and the true posterior (Blei and Lafferty (2007); Hinton and Van Camp (1993)) as

$$\pi^* = \underset{q \in \mathcal{Q}^{\text{MF}}}{\text{argmin}} d_{\text{KL}}(q, \pi(|\mathcal{D})) \quad (8)$$

where $d_{\text{KL}}(q, \pi(|\mathcal{D}))$ denotes the KL-distance between q and $\pi(|\mathcal{D})$.

Note, the variational member q can be written as $q(\boldsymbol{\theta}, \mathbf{z}) = q(\boldsymbol{\theta}|\mathbf{z})q(\mathbf{z})$ where $q(\mathbf{z})$ is the probability mass function of \mathbf{z} with respect to the counting measure and $q(\boldsymbol{\theta}|\mathbf{z})$ is the conditional density function given with respect to the Lebesgue measure of $\boldsymbol{\theta}$ given \mathbf{z} . Further,

$$\begin{aligned} \pi^* &= \operatorname{argmin}_{q \in \mathcal{Q}^{\text{MF}}} \sum_{\mathbf{z}} \int [\log q(\boldsymbol{\theta}, \mathbf{z}) - \log \pi(\boldsymbol{\theta}, \mathbf{z}|\mathcal{D})] q(\boldsymbol{\theta}, \mathbf{z}) d\boldsymbol{\theta} \\ &= \operatorname{argmin}_{q \in \mathcal{Q}^{\text{MF}}} \left(\sum_{\mathbf{z}} \int [\log q(\boldsymbol{\theta}, \mathbf{z}) - \log \pi(\boldsymbol{\theta}, \mathbf{z}, \mathcal{D})] q(\boldsymbol{\theta}, \mathbf{z}) d\boldsymbol{\theta} + \log m(\mathcal{D}) \right) \\ &= \operatorname{argmin}_{q \in \mathcal{Q}^{\text{MF}}} [-\text{ELBO}(q, \pi(|\mathcal{D}|))] + \log m(\mathcal{D}) = \operatorname{argmax}_{q \in \mathcal{Q}^{\text{MF}}} \text{ELBO}(q, \pi(|\mathcal{D}|)) \end{aligned} \quad (9)$$

Since $\log m(\mathcal{D})$ is free from q , it suffices to maximize the evidence lower bound (ELBO) above.

Let $\tilde{\pi}^*(\boldsymbol{\theta}) = \sum_{\mathbf{z}} \pi^*(\boldsymbol{\theta}|\mathbf{z})\pi^*(\mathbf{z})$ then $\tilde{\pi}^*$ denotes the marginal variational posterior for $\boldsymbol{\theta}$. We shall use the notation

$$\tilde{\Pi}^*(\mathcal{A}) = \int_{\mathcal{A}} \tilde{\pi}^*(\boldsymbol{\theta}) d\boldsymbol{\theta} \quad (10)$$

to denote the probability distribution function corresponding to the density function $\tilde{\pi}^*$.

4 Posterior contraction rates

In this section, we develop the theoretical consistency of variational posterior under three network related assumptions (1) the number of nodes in the model may vary with the layer index (2) the best neural network approximation to the function η_0 may have varying number of nodes in each layer (3) the best neural network approximation to the function η_0 may have varying bounds on the L_1 norm of the incoming weights (including the bias term) onto the node for each layer. Previous works which establish the statistical consistency of sparse deep neural networks do so only in the context of edge selection. Thereby, the works of Polson and Ročková (2018), Chérif-Abdellatif (2020) and Bai et al. (2020) use several results from the pioneer work of Schmidt-Hieber (2020). These prior works only provide statistical guarantees for sparse networks which may or may not be structurally sparse. In contrast pruning away multiple nodes from a given network does guarantee a structurally sparse solution. Further, the previous works assume an equal number of nodes in each layer which restricts one from using any previous information on the number of nodes in the deep neural architecture. Finally, all these works assume a known bound B on all the neural network weights as they essentially rely on the sieve construction in equation 3 of Schmidt-Hieber (2020) which assumes that L_∞ norm of all $\boldsymbol{\theta}$ entries is smaller than 1.

In our current work, we provide the statistical guarantees for structurally sparse neural network solutions. Further, we allow such sparse network to have varying number of nodes in each layer. We relax the assumption of known bound B on all the coefficients. Also, instead of a unified sparsity in the overall network indexed by s (see the sieve construction in relation (4) of Schmidt-Hieber (2020)) we allow for layer wise sparsity vector \mathbf{s} to account for the number of nodes in each layer. In addition to the sparsity vector \mathbf{s} , we also assume a layer wise L_1 norm constraint vector \mathbf{B} on the incoming edges of a node. Thus, our work extends on current literature along three directions (1) theoretically quantifies predictive performance of Bayesian neural networks with node based pruning (2) establishes that even without a fixed bound on network weights, one can recover true solution by appropriate choice of the prior (3) provides layer wise node inclusion probabilities to allow for structurally sparse solutions. The relaxation of these network structure assumptions requires us to provide the framework for node selection including appropriate sieve construction together with the derivation of the results in Schmidt-Hieber (2020) customized to our problem.

To establish the posterior contraction rates, we show that the variational posterior in (8) concentrates

in shrinking Hellinger neighborhoods of the true density function P_0 with overwhelming probability. Since $\mathbf{X} \sim U[0, 1]^p$, thus $f_0(\mathbf{x}) = f_\theta(\mathbf{x}) = 1$. This further implies $P_0 = f_0(y|\mathbf{x})f_0(\mathbf{x}) = f_0(y|\mathbf{x})$ and similarly $P_\theta = f_\theta(y|\mathbf{x})$. We next define the Hellinger neighborhood of the true density P_0 as

$$\mathcal{H}_\varepsilon = \{\theta : d_H(P_0, P_\theta) < \varepsilon\}$$

where the Hellinger distance between the true density function P_0 and the model density P_θ is

$$d_H^2(P_0, P_\theta) = \frac{1}{2} \int \left(\sqrt{f_\theta(y|\mathbf{x})} - \sqrt{f_0(y|\mathbf{x})} \right)^2 dy d\mathbf{x}$$

We also define the KL neighborhood of the true density P_0 as

$$\mathcal{N}_\varepsilon = \{\theta : d_{\text{KL}}(P_0, P_\theta) < \varepsilon\}$$

where the KL distance d_{KL} between the true density function P_0 and the model density P_θ is

$$d_{\text{KL}}(P_0, P_\theta) = \int \log \frac{f_0(y|\mathbf{x})}{f_\theta(y|\mathbf{x})} f_0(y|\mathbf{x}) dy d\mathbf{x}$$

Let $\mathbf{k} = (k_0, \dots, k_{L+1})$ be the node vector, $\overline{\mathbf{W}}_l = (\mathbf{w}_{l1}^\top, \dots, \mathbf{w}_{lk_{l+1}}^\top)^\top$ be the row representation of $\overline{\mathbf{W}}_l$ and $\tilde{\mathbf{w}}_l = (\|\mathbf{w}_{l1}\|_1, \dots, \|\mathbf{w}_{lk_{l+1}}\|_1)$ be the vector of L_1 norms of the rows of $\overline{\mathbf{W}}_l$. Next we consider layer-wise sparsity, $\mathbf{s} = (s_1, \dots, s_L)$ for node selection. Similarly, we consider layer-wise norm constraints, $\mathbf{B} = (B_1, \dots, B_L)$ on L_1 norms of weights including bias incident onto any given node in each layer. Based on \mathbf{s} and \mathbf{B} , we define the following sieve of neural networks (check definition A.1).

$$\mathcal{F}(L, \mathbf{k}, \mathbf{s}, \mathbf{B}) = \{\eta_\theta \in (3) : \|\tilde{\mathbf{w}}_l\|_0 \leq s_l, \|\tilde{\mathbf{w}}_l\|_\infty \leq B_l\}. \quad (11)$$

The construction of a sieve is one of the most important tools towards the proof of consistency in infinite-dimensional spaces. In the works of Schmidt-Hieber (2020), Polson and Ročková (2018), Chérif-Abdellatif (2020) and Bai et al. (2020), the sieve in the context of edge selection is given by

$$\mathcal{F}(L, \mathbf{k}, s) = \{\eta_\theta \in (3) : \|\theta\|_0 \leq s, \|\theta\|_\infty \leq 1\}.$$

which works with an overall sparsity parameter s . In addition, note the L_∞ norm of all the entries in θ is assumed to be known constant equal to 1 (see relation (4) in Schmidt-Hieber (2020) and section 4 in Polson and Ročková (2018)). Section 3 in Bai et al. (2020) does not explicitly mention the dependence of their sieve on some fixed bound B on the edges in a network, however, their derivations on covering numbers (see proof of Lemma 1.2 in the supplement of Bai et al. (2020)) borrow results from Schmidt-Hieber (2020) which is based on sieve with $B = 1$.

Consider any sequence ϵ_n . For Lemmas 4.1 and 4.2, we work with the sieve $\mathcal{F}(L, \mathbf{k}, \mathbf{s}, \mathbf{B})$ in (11) with $\mathbf{s} = \mathbf{s}^\circ$ and $\mathbf{B} = \mathbf{B}^\circ$ where $s_l^\circ + 1 = n\epsilon_n^2 / (\sum_{j=0}^L u_j)$ and $\log B_l^\circ = (n\epsilon_n^2) / ((L+1) \sum_{j=0}^L (s_j^\circ + 1))$ with $u_l = (L+1)^2 (\log n + \log(L+1) + \log k_{l+1} + \log(k_l + 1))$. Note, s_l° and B_l° do not depend on l .

Lemma 4.1 below holds when the covering number (check definition A.2) of the functions which belong to the sieve $\mathcal{F}(L, \mathbf{k}, \mathbf{s}^\circ, \mathbf{B}^\circ)$ is well under control. Lemma 4.2 below states that for the same choice of the sieve, the prior gives sufficiently small probabilities on the complement space $\mathcal{F}(L, \mathbf{k}, \mathbf{s}^\circ, \mathbf{B}^\circ)^c$ (see the discussion under Theorem 4.4 for more details).

For the subsequent results, the symbol \mathcal{A}^c will be used to denote complement of a set \mathcal{A} .

Lemma 4.1 (Existence of Test Functions). *Let $\epsilon_n \rightarrow 0$ and $n\epsilon_n^2 \rightarrow \infty$. There exists a testing function*

$\phi \in [0, 1]$ and constants $C_1, C_2 > 0$,

$$\begin{aligned} \mathbb{E}_{P_0}(\phi) &\leq \exp\{-C_1 n \epsilon_n^2\} \\ \sup_{\boldsymbol{\theta} \in \mathcal{H}_{\epsilon_n}, \eta_{\boldsymbol{\theta}} \in \mathcal{F}(L, \mathbf{k}, \mathbf{s}^\circ, \mathbf{B}^\circ)} \mathbb{E}_{P_{\boldsymbol{\theta}}}(1 - \phi) &\leq \exp\{-C_2 n d_{\text{H}}^2(P_0, P_{\boldsymbol{\theta}})\} \end{aligned}$$

where $\mathcal{H}_{\epsilon_n} = \{\boldsymbol{\theta} : d_{\text{H}}(P_0, P_{\boldsymbol{\theta}}) \leq \epsilon_n\}$ is the Hellinger neighborhood of radius ϵ_n .

Lemma 4.2 (Prior mass condition.). *Let $\epsilon_n \rightarrow 0$, $n\epsilon_n^2 \rightarrow \infty$ and $n\epsilon_n^2 / \sum_{l=0}^L u_l \rightarrow \infty$, then for $\tilde{\Pi}$ as in (6) and some constant $C_3 > 0$,*

$$\tilde{\Pi}(\mathcal{F}(L, \mathbf{k}, \mathbf{s}^\circ, \mathbf{B}^\circ)^c) \leq \exp(-C_3 n \epsilon_n^2 / \sum_{l=0}^L u_l)$$

Whereas Lemmas 4.1 and 4.2 work with a specific choice of the sieve, the following Lemma 4.3 is developed for any generic choice of sieve indexed by \mathbf{s} and \mathbf{B} . The final piece of the theory developed next tries to address two main questions (1) Can we get a sparse network solution whose layer-wise sparsity levels and L_1 norms of incident edges (including the bias) of the nodes are controlled at levels \mathbf{s} and \mathbf{B} respectively? (2) Does this sparse network retain the same predictive performance as the original network?

In this direction, let

$$\xi = \min_{\eta_{\boldsymbol{\theta}} \in \mathcal{F}(L, \mathbf{k}, \mathbf{s}, \mathbf{B})} \|\eta_{\boldsymbol{\theta}} - \eta_0\|_\infty^2$$

Based on the values \mathbf{s} and \mathbf{B} , we also define

$$\begin{aligned} \vartheta_l &= B_l^2 / (k_l + 1) + \sum_{m=0, m \neq l}^L \log B_m + L + \log k_{l+1} + \log(k_l + 1) + \log n + \log\left(\sum_{m=0}^L u_m\right) \\ r_l &= s_l(k_l + 1)\vartheta_l / n \end{aligned} \tag{12}$$

Lemma 4.3 has two sub conditions. Condition 1. requires that shrinking KL neighborhood of the true density function P_0 gets sufficiently large probability. This along with Lemma 4.1 and 4.2 is an essential condition to guarantee the convergence of the true posterior in (5). Condition 2. is the assumption needed to control the KL distance between true posterior and variational posterior and thereby guarantees the convergence of the variational posterior in (8) (see the discussion under Theorem 4.4 for more details).

Lemma 4.3 (Kullback-Leibler conditions). *Suppose $\sum_{l=0}^L r_l + \xi \rightarrow 0$ and $n(\sum_{l=0}^L r_l + \xi) \rightarrow \infty$ and the following two conditions hold for the prior $\tilde{\Pi}$ in (6) and some $q \in \mathcal{Q}^{\text{MF}}$*

1. $\tilde{\Pi}\left(\mathcal{N}_{\sum_{l=0}^L r_l + \xi}\right) \geq \exp(-C_4 n(\sum_{l=0}^L r_l + \xi))$
2. $d_{\text{KL}}(q, \pi) + n \sum_{\mathbf{z}} \int d_{\text{KL}}(P_0, P_{\boldsymbol{\theta}}) q(\boldsymbol{\theta}, \mathbf{z}) d\boldsymbol{\theta} \leq C_5 n(\sum_{l=0}^L r_l + \xi)$

where π is the joint prior of $(\boldsymbol{\theta}, \mathbf{z})$, q is the joint variational distribution of $(\boldsymbol{\theta}, \mathbf{z})$ and $\mathcal{N}_{\sum_{l=0}^L r_l + \xi}$ is the KL neighborhood of radius $\sum_{l=0}^L r_l + \xi$.

The following result shows that the variational posterior is consistent as long as Lemma 4.1, Lemma 4.2 and Lemma 4.3 hold. The proof of Theorem 4.4 demonstrates how the validity of these three lemmas imply variational posterior consistency.

Theorem 4.4. *Suppose Lemma 4.3 holds and Lemmas 4.1 and 4.2 hold for $\epsilon_n = \sqrt{(\sum_{l=0}^L r_l + \xi) \sum_{l=0}^L u_l}$. Then for some slowly increasing sequence $M_n \rightarrow \infty$, $M_n \epsilon_n \rightarrow 0$ and $\tilde{\Pi}^*$ as in (10),*

$$\tilde{\Pi}^*(\mathcal{H}_{M_n \epsilon_n}^c) \rightarrow 0, \quad n \rightarrow \infty$$

in P_0^n probability where $\mathcal{H}_{M_n \epsilon_n}^c = \{\boldsymbol{\theta} : d_H(P_0, P_{\boldsymbol{\theta}}) \leq M_n \epsilon_n\}$ is the Hellinger neighborhood of radius $M_n \epsilon_n$.

Note, the above contraction rate depends mainly on two quantities r_l and ξ . Note r_l controls the number of nodes in the neural network. If the network is not sparse, then r_l is $k_{l+1}(k_l + 1)\vartheta_l/n$ instead of $s_l(k_l + 1)\vartheta_l/n$ which can in turn make the convergence of $\epsilon_n \rightarrow 0$ difficult. On the other hand, if s_l and B_l are too small, it will cause ξ to explode since a good approximation to the true function may not exist in a very sparse space.

Remark (Rates as a function of n). *Let $L \sim O(\log n)$, $B_l^2 \sim O(k_l + 1)$ and $s_l(k_l + 1) = O(n^{1-2\rho})$, for some $\rho > 0$, then one can work with $\epsilon_n = n^{-\rho} \log^3(n)$ as long as $\xi = O(n^{-2\rho} \log^2(n))$. The exact expression of ρ is determined by the degree of smoothness of the function η_0 .*

Proof of Theorem 4.4

Discussion. To further enunciate Lemmas 4.1 and 4.2 consider the quantity $\mathcal{E}_{1n} = \int_{\mathcal{H}_{M_n \epsilon_n}^c} (P_{\boldsymbol{\theta}}^n/P_0^n) \tilde{\pi}(\boldsymbol{\theta}) d\boldsymbol{\theta}$ as used in the following proof. Here, \mathcal{E}_{1n} can be split into two parts

$$\mathcal{E}_{1n} = \int_{\mathcal{H}_{M_n \epsilon_n}^c \cap \mathcal{F}(L, \mathbf{k}, \mathbf{s}^\circ, \mathbf{B}^\circ)} (P_{\boldsymbol{\theta}}^n/P_0^n) \tilde{\pi}(\boldsymbol{\theta}) d\boldsymbol{\theta} + \int_{\mathcal{H}_{M_n \epsilon_n}^c \cap \mathcal{F}(L, \mathbf{k}, \mathbf{s}^\circ, \mathbf{B}^\circ)^c} (P_{\boldsymbol{\theta}}^n/P_0^n) \tilde{\pi}(\boldsymbol{\theta}) d\boldsymbol{\theta}$$

Whereas Lemma 4.1 provides a handle on the first term by controlling the covering number of the sieve $\mathcal{F}(L, \mathbf{k}, \mathbf{s}^\circ, \mathbf{B}^\circ)$, Lemma 4.2 gives a handle on the second term by controlling $\tilde{\Pi}(\mathcal{F}(L, \mathbf{k}, \mathbf{s}^\circ, \mathbf{B}^\circ)^c)$ (for more details we refer to Lemma A.8 in the Appendix A).

Next, consider the quantity $\mathcal{E}_{2n} = \log \int (P_{\boldsymbol{\theta}}^n/P_0^n) \tilde{\pi}(\boldsymbol{\theta}) d\boldsymbol{\theta}$ in the following proof. Lemma 4.3 part 1. provides a control on this term (see Lemma A.9 in the the Appendix A for more details). Finally, consider the quantity $\mathcal{E}_{3n} = d_{\text{KL}}(q, \pi) + \sum_{\mathbf{z}} \int \log(P_0^n/P_{\boldsymbol{\theta}}^n) q(\boldsymbol{\theta}, \mathbf{z}) d\boldsymbol{\theta}$ in the following proof. Indeed Lemma 4.3 part 2. provides a control on this term (see Lemma A.10 in the Appendix A for further details).

Proof. Let $\tilde{\Pi}$ and $\tilde{\Pi}^*$ be as in (7) and (10) respectively. Now,

$$\begin{aligned} d_{\text{KL}}(\tilde{\pi}^*, \tilde{\pi}(|\mathcal{D})) &= \int_{\mathcal{A}} \tilde{\pi}^*(\boldsymbol{\theta}) \log \frac{\tilde{\pi}^*(\boldsymbol{\theta})}{\tilde{\pi}(\boldsymbol{\theta}|\mathcal{D})} d\boldsymbol{\theta} + \int_{\mathcal{A}^c} \tilde{\pi}^*(\boldsymbol{\theta}) \log \frac{\tilde{\pi}^*(\boldsymbol{\theta})}{\tilde{\pi}(\boldsymbol{\theta}|\mathcal{D})} d\boldsymbol{\theta} \\ &= -\tilde{\Pi}^*(\mathcal{A}) \int_{\mathcal{A}} \frac{\tilde{\pi}^*(\boldsymbol{\theta})}{\tilde{\Pi}^*(\mathcal{A})} \log \frac{\tilde{\pi}(\boldsymbol{\theta}|\mathcal{D})}{\tilde{\pi}^*(\boldsymbol{\theta})} d\boldsymbol{\theta} - \tilde{\Pi}^*(\mathcal{A}^c) \int_{\mathcal{A}^c} \frac{\tilde{\pi}^*(\boldsymbol{\theta})}{\tilde{\Pi}^*(\mathcal{A}^c)} \log \frac{\tilde{\pi}(\boldsymbol{\theta}|\mathcal{D})}{\tilde{\pi}^*(\boldsymbol{\theta})} d\boldsymbol{\theta} \\ &\geq \tilde{\Pi}^*(\mathcal{A}) \log \frac{\tilde{\Pi}^*(\mathcal{A})}{\tilde{\Pi}(\mathcal{A}|\mathcal{D})} + \tilde{\Pi}^*(\mathcal{A}^c) \log \frac{\tilde{\Pi}^*(\mathcal{A}^c)}{\tilde{\Pi}(\mathcal{A}^c|\mathcal{D})}, \quad \text{Jensen's inequality} \end{aligned}$$

where the above lines hold for any set \mathcal{A} . Since $\tilde{\Pi}(\mathcal{A}|\mathcal{D}) \leq 1$,

$$\begin{aligned} &\geq \tilde{\Pi}^*(\mathcal{A}) \log \tilde{\Pi}^*(\mathcal{A}) + \tilde{\Pi}^*(\mathcal{A}^c) \log \tilde{\Pi}^*(\mathcal{A}^c) - \tilde{\Pi}^*(\mathcal{A}^c) \log \tilde{\Pi}(\mathcal{A}^c|\mathcal{D}) \\ &\geq -\tilde{\Pi}^*(\mathcal{A}^c) \log \tilde{\Pi}(\mathcal{A}^c|\mathcal{D}) - \log 2, \quad (\because x \log x + (1-x) \log(1-x) \geq -\log 2) \\ &= -\tilde{\Pi}^*(\mathcal{A}^c) \left(\underbrace{\log \int_{\mathcal{A}^c} (P_{\boldsymbol{\theta}}^n/P_0^n) \tilde{\pi}(\boldsymbol{\theta}) d\boldsymbol{\theta}}_{\mathcal{E}_{1n}} - \underbrace{\log \int (P_{\boldsymbol{\theta}}^n/P_0^n) \tilde{\pi}(\boldsymbol{\theta}) d\boldsymbol{\theta}}_{\mathcal{E}_{2n}} \right) - \log 2 \end{aligned}$$

The above representation is similar to the proof of Theorems 3.1 and 3.2 in Bhattacharya and Maiti (2021).

For any $q \in \mathcal{Q}^{\text{MF}}$,

$$\begin{aligned}
-\tilde{\Pi}^*(\mathcal{A}^c)\mathcal{E}_{1n} &\leq d_{\text{KL}}(\tilde{\pi}^*, \tilde{\pi}(|\mathcal{D})) - \tilde{\Pi}^*(\mathcal{A}^c)\mathcal{E}_{2n} + \log 2 \\
&\leq d_{\text{KL}}(\pi^*, \pi(|\mathcal{D})) - \tilde{\Pi}^*(\mathcal{A}^c)\mathcal{E}_{2n} + \log 2 && \text{by Lemma A.5} \\
&\leq d_{\text{KL}}(q, \pi(|\mathcal{D})) - \tilde{\Pi}^*(\mathcal{A}^c)\mathcal{E}_{2n} + \log 2 && \pi^* \text{ is the KL minimizer} \\
&\leq \underbrace{d_{\text{KL}}(q, \pi) + \sum_{\mathbf{z}} \int \log \frac{P_0^n}{P_{\boldsymbol{\theta}}^n} q(\boldsymbol{\theta}, \mathbf{z}) d\boldsymbol{\theta}}_{\mathcal{E}_{3n}} + (1 - \tilde{\Pi}^*(\mathcal{A}^c))\mathcal{E}_{2n} + \log 2 \\
&= \mathcal{E}_{3n} + (1 - \tilde{\Pi}^*(\mathcal{A}^c))\mathcal{E}_{2n} + \log 2
\end{aligned} \tag{13}$$

where the fourth inequality in the above equation follows since

$$\begin{aligned}
d_{\text{KL}}(q, \pi(|\mathcal{D})) &= \sum_{\mathbf{z}} \int (\log q(\boldsymbol{\theta}, \mathbf{z}) - \log P_{\boldsymbol{\theta}}^n - \log \pi(\boldsymbol{\theta}, \mathbf{z}) + \log m(\mathcal{D})) q(\boldsymbol{\theta}, \mathbf{z}) d\boldsymbol{\theta} \\
&= \underbrace{\sum_{\mathbf{z}} \int (\log q(\boldsymbol{\theta}, \mathbf{z}) - \log \pi(\boldsymbol{\theta}, \mathbf{z})) q(\boldsymbol{\theta}, \mathbf{z}) d\boldsymbol{\theta}}_{d_{\text{KL}}(q, \pi)} + \sum_{\mathbf{z}} \int (\log P_0^n - \log P_{\boldsymbol{\theta}}^n) q(\boldsymbol{\theta}, \mathbf{z}) d\boldsymbol{\theta} \\
&\quad + \underbrace{\log m(\mathcal{D}) - \log P_0^n}_{\mathcal{E}_{2n}}
\end{aligned}$$

where $m(\mathcal{D})$ is the marginal distribution of data as in (5).

Take $\mathcal{A} = \mathcal{H}_{M_n \epsilon_n}^c = \{\boldsymbol{\theta} : d_{\text{H}}(P_0, P_{\boldsymbol{\theta}}) > M_n \epsilon_n\}$

If Lemma 4.1 and 4.2 hold, then by Lemma A.8, it can be shown that $\mathcal{E}_{1n} \leq -nC M_n^2 \epsilon_n^2 / \sum u_l$ for any $M_n \rightarrow \infty$ with high probability.

If Lemma 4.3 condition 1. holds, then by Lemma A.9, $\mathcal{E}_{2n} \leq nM_n(\sum_{l=0}^L r_l + \xi)$ for any $M_n \rightarrow \infty$.

If Lemma 4.3 condition 2. hold, then by Lemma A.10, $\mathcal{E}_{3n} \leq nM_n(\sum_{l=0}^L r_l + \xi)$ for any $M_n \rightarrow \infty$.

Therefore, by (13), we get

$$\begin{aligned}
\frac{nC M_n^2 \epsilon_n^2}{\sum u_l} \tilde{\Pi}^*(\mathcal{H}_{M_n \epsilon_n}^c) &\leq nM_n \left(\sum_{l=0}^L r_l + \xi \right) + nM_n \left(\sum_{l=0}^L r_l + \xi \right) + \log 2 \\
&\leq nM_n \left(\sum_{l=0}^L r_l + \xi \right) + nM_n \left(\sum_{l=0}^L r_l + \xi \right) + M_n \left(\sum_{l=0}^L r_l + \xi \right) \\
\implies \tilde{\Pi}^*(\mathcal{H}_{M_n \epsilon_n}^c) &\leq \frac{3M_n(\sum_{l=0}^L r_l + \xi) \sum u_l}{C_1 M_n^2 \epsilon_n^2}
\end{aligned}$$

Taking $\epsilon_n = \sqrt{\sum_{l=0}^L (r_l + \xi) \sum u_l}$ and noting $M_n \rightarrow \infty$, the proof follows. \square

We next give conditions on the prior probabilities λ_l and σ_0 to guarantee that Lemmas 4.1, 4.2 and 4.3 hold. This in turn implies the conditions of Theorem 4.4 hold and variational posterior is consistent.

Corollary 4.5. *Let $\sigma_0^2 = 1$, $-\log \lambda_l = \log(k_{l+1}) + C_l(k_l + 1)\vartheta_l$, then conditions of Theorem 4.4 hold and $\tilde{\Pi}^*$ as in (10) satisfies*

$$\tilde{\Pi}^*(\mathcal{H}_{M_n \epsilon_n}^c) \rightarrow 0, \quad n \rightarrow \infty$$

in P_0^n probability where and $\mathcal{H}_{M_n \epsilon_n} = \{\boldsymbol{\theta} : d_{\text{H}}(P_0, P_{\boldsymbol{\theta}}) \leq M_n \epsilon_n\}$ is the Hellinger neighborhood of radius $M_n \epsilon_n$.

The proof of the corollary has been provided in Appendix A.

In the preceding corollary, note that our expression of prior inclusion probability varies as a function of l thereby providing a handle on layer-wise sparsity. Indeed, using these expressions in numerical studies further substantiates the theoretical framework developed in this section.

Remark (Optimal Contraction). *For a fixed choice of \mathbf{k} , the optimal contraction rate is achieved at \mathbf{s}^* , $\mathbf{B}^* = \operatorname{argmin}_{\mathbf{s}, \mathbf{B}} (\sum r_l + \xi)$. Thus, \mathbf{s}^* and \mathbf{B}^* are the optimal values of \mathbf{s} and \mathbf{B} which give the best sparse network with minimal loss in the true accuracy. The corresponding probability expressions in Corollary 4.5 can be accordingly modified by setting $\mathbf{s} = \mathbf{s}^*$ and $\mathbf{B} = \mathbf{B}^*$ in the expressions of ϑ_l and r_l in (12).*

5 Implementation Details

Evidence Lower Bound. The ELBO presented in (9) is given by $\mathcal{L} = -E_q[\log P_{\boldsymbol{\theta}}^n] + d_{\text{KL}}(q, \pi)$ which is further simplified as

$$\begin{aligned}
& -E_q[\log P_{\boldsymbol{\theta}}^n] + d_{\text{KL}}(q, \pi) \\
&= -\mathbb{E}_{q(\boldsymbol{\theta}|\mathbf{z})q(\mathbf{z})}[\log P_{\boldsymbol{\theta}}^n] + d_{\text{KL}}(q(\boldsymbol{\theta}|\mathbf{z})q(\mathbf{z}), \pi(\boldsymbol{\theta}|\mathbf{z})\pi(\mathbf{z})) \\
&= -\mathbb{E}_{q(\boldsymbol{\theta}|\mathbf{z})q(\mathbf{z})}[\log P_{\boldsymbol{\theta}}^n] + \sum_{l,j} d_{\text{KL}}(q(z_{lj})||\pi(z_{lj})) \\
&\quad + \sum_{l,j} [q(z_{lj} = 1)d_{\text{KL}}(q(\bar{\mathbf{w}}_{lj}|z_{lj} = 1)||\pi(\bar{\mathbf{w}}_{lj}|z_{lj} = 1)) + q(z_{lj} = 0)d_{\text{KL}}(q(\bar{\mathbf{w}}_{lj}|z_{lj} = 0)||\pi(\bar{\mathbf{w}}_{lj}|z_{lj} = 0))] \\
&= -\mathbb{E}_{q(\boldsymbol{\theta}|\mathbf{z})q(\mathbf{z})}[\log P_{\boldsymbol{\theta}}^n] + \sum_{l,j} d_{\text{KL}}(q(z_{lj})||\pi(z_{lj})) + \sum_{l,j} q(z_{lj} = 1)d_{\text{KL}}(q(\bar{\mathbf{w}}_{lj}|z_{lj} = 1)||\pi(\bar{\mathbf{w}}_{lj}|z_{lj} = 1)) \\
&= -\mathbb{E}_{q(\boldsymbol{\theta}|\mathbf{z})q(\mathbf{z})}[\log P_{\boldsymbol{\theta}}^n] + \sum_{l,j} d_{\text{KL}}(q(z_{lj})||\pi(z_{lj})) + \sum_{l,j} q(z_{lj} = 1)d_{\text{KL}}(N(\boldsymbol{\mu}_{lj}, \operatorname{diag}(\boldsymbol{\sigma}_{lj}^2))||N(0, \sigma_0^2 \mathbf{I}))
\end{aligned}$$

The KL of discrete variables appearing in the above expression creates a challenge in practical implementation. Jang et al. (2017), Maddison et al. (2017) proposed to replace discrete random variable with its continuous relaxation. Specifically, the continuous relaxation approximation is achieved through Gumbel-softmax (GS) distribution, that is $q(z_{lj}) \sim \operatorname{Ber}(\gamma_{lj})$ is approximated by $q(\tilde{z}_{lj}) \sim \operatorname{GS}(\gamma_{lj}, \tau)$, where

$$\tilde{z}_{lj} = (1 + \exp(-\eta_{lj}/\tau))^{-1}, \quad \eta_{lj} = \log(\gamma_{lj}/(1 - \gamma_{lj})) + \log(u_{lj}/(1 - u_{lj})), \quad u_{lj} \sim U(0, 1)$$

where τ is the temperature. We set $\tau = 0.5$ for this paper (also see section 5 in Bai et al. (2020)). \tilde{z}_{lj} is used in the backward pass for easier gradient calculation, while z_{lj} will be used for selecting nodes in the forward pass. We use non-centered parameterization for the Gaussian slab variational approximation where $N(\boldsymbol{\mu}_{lj}, \operatorname{diag}(\boldsymbol{\sigma}_{lj}^2))$ is reparameterized as $\boldsymbol{\mu}_{lj} + \boldsymbol{\sigma}_{lj} \odot \boldsymbol{\zeta}_{lj}$ for $\boldsymbol{\zeta}_{lj} \sim N(0, \mathbf{I})$, where \odot denotes the entry-wise (Hadamard) product.

Algorithm 1 Variational inference in SS-IG Bayesian neural networks

Inputs: training dataset, network architecture, and optimizer tuning parameters.

Model inputs: prior parameters for θ, z .

Variational inputs: number of Monte Carlo samples S .

Output: Variational parameter estimates of network weights and sparsity.

Method: Set initial values of variational parameters.

repeat

 Generate S samples from $\zeta_{lj} \sim N(0, \mathbf{I})$ and $u_{lj} \sim U(0, 1)$

 Generate S samples for (z_{lj}, \tilde{z}_{lj}) using u_{lj}

 Use $\mu_{lj}, \sigma_{lj}, \zeta_{lj}$ and z_{lj} to compute loss (ELBO) in forward pass

 Use $\mu_{lj}, \sigma_{lj}, \zeta_{lj}$ and \tilde{z}_{lj} to compute gradient of loss in backward pass

 Update the variational parameters with gradient of loss using stochastic gradient descent algorithm (e.g. Adam (Kingma and Ba, 2015))

until change in ELBO $< \epsilon$

6 Numerical Experiments

In this section, we present several numerical experiments to demonstrate the performance of our spike-and-slab independent Gaussian (SS-IG) Bayesian neural networks which we implement in PyTorch (Paszke et al., 2019). Further, to evaluate the efficacy of the variational inference we benchmark our model on synthetic as well as real datasets. Our numerical investigation justifies the use of proposed choices of prior hyperparameters specifically layer-wise prior inclusion probabilities, which in turn substantiates the significance of our theoretical developments. With the fully Bayesian treatment, we are also able to quantify the uncertainties for the parameter estimates and variational inference helps us to scale our model to large datasets.

We compare our sparse model with a node selection technique-horseshoe BNN (HS-BNN) (Ghosh et al., 2019) and an edge selection technique-spike-and-slab BNN (SV-BNN) (Bai et al., 2020) in the second simulation study and UCI regression dataset examples. We use optimal choices of prior parameters and fine tuning parameters provided by the authors of HS-BNN and SV-BNN in their respective models. Further we compare our model against dense variational BNN model (VBNN) (Blundell et al., 2015) in all of the experiments. Since it has no sparse structure, it serves as a baseline allowing to check whether sparsity compromises accuracy. In all the experiments, we fix $\sigma_0^2 = 1$ and $\sigma_e^2 = 1$. For our model, the choices of layer-wise λ_l follow from Corollary 4.5: $\lambda_l = (1/k_{l+1}) \exp(-C_l(k_l + 1)\vartheta_l)$. We take C_l values in the negative order of 10 such that prior inclusion probabilities do not fall below 10^{-50} otherwise λ_l values close to 0 might prune away all the nodes from a layer (check appendix B for more discussion). The remaining tuning parameter details such as learning rate, minibatch size, and initial parameter choice are provided in the appendix B. The prediction accuracy is calculated using variational Bayes posterior mean estimator with 30 Monte Carlo samples in testing phase.

6.1 Simulation Study - I

We consider a two dimensional regression problem where the true response y_0 is generated by sampling X from $U([-1, 1]^2)$ and feeding it to a deep neural network with known parameters. We add a random Gaussian noise with $\sigma = 5\% \sqrt{\text{Var}(y_0)}$ to y_0 to get noisy outputs y . We create the dataset using a shallow neural network consisting of 2 inputs, one hidden layer with 2 nodes and 1 output (2-2-1 network). We train our SS-IG model and VBNN model using a single hidden layer network with 20 neurons in the hidden layer and administer sigmoid activation. Each model is trained till convergence. We found that both models give

competitive predictive performance while fitting the given data. In Figure 2 we plot the magnitudes of the incoming weights into the hidden layer nodes using boxplots. Our model with the help of spike and slab prior is able to prune away redundant nodes not required for fitting the model. Since VBNN is densely connected, it shows all the nodes being active in its final model. From this experiment, it is clear that neural networks can be pruned leading to more compact models at inference stage without compromising the accuracy. We also performed the same experiment with a wider neural network consisting of 100 nodes in the single hidden layer and provide the results in the appendix B. There again we show that our model can easily recover very sparse solution with competitive predictive performance.

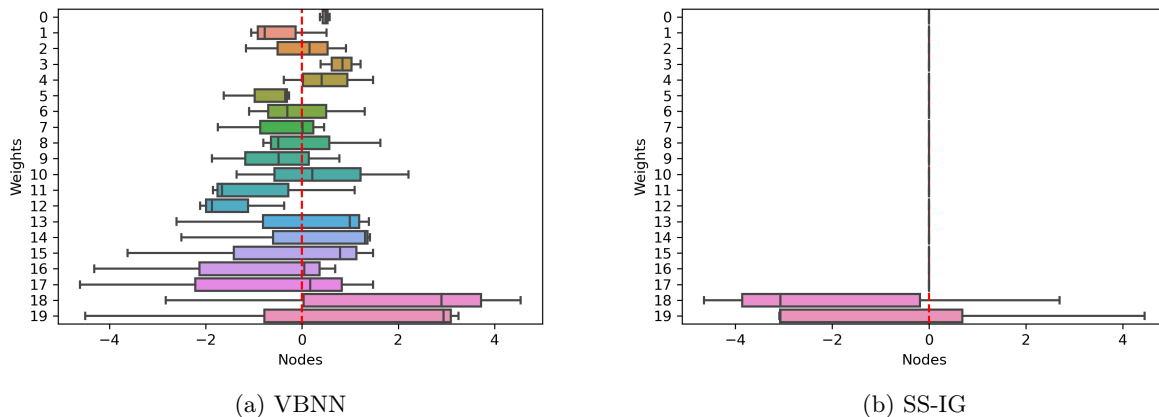


Figure 2: Node-wise weight magnitudes recovered by VBNN and proposed SS-IG model in the synthetic regression data generated using 2-2-1 network. The boxplots show the distribution of incoming weights into a given hidden layer node.

6.2 Simulation Study - II

We consider a nonlinear regression example where we generate the data from the following model:

$$y = \frac{7x_2}{1 + x_1^2} + \sin(x_3x_4) + 2x_5 + \varepsilon,$$

where $\varepsilon \sim N(0, 1)$. Further all the covariates are i.i.d. $N(0, 1)$ and independent of ε . We generated 3000 data entries to create the training data for the experiment. Additional 1000 observations were generated for testing. We modeled this data using 2-hidden layer neural network which consists of 20 neurons per hidden layer. Sigmoid activation function is administered for each model used for comparative analysis. Table 1 illustrates the predictive performance of our model compared to SV-BNN, HS-BNN, and VBNN models. Our model is extremely well at pruning redundant nodes which leads to the most compact model compared to the other sparse models: SV-BNN and HS-BNN. Moreover it exhibits lower root mean squared error (RMSE) values among the sparse models while showing similar predictive performance compared to the densely connected VBNN. This experiment further underscores the major utility of our model to generate very compact models which could reduce computational times and memory usage at inference stage.

Table 1: Performance of the proposed SS-IG, SV-BNN, HS-BNN, and VBNN models in simulation study II. Each model was trained for 10k epochs with learning rate 5×10^{-3} . Mean and S.D. of RMSE values and median sparsity estimates were calculated from last 1000 epochs (with jump of 10 giving us sample of 100).

Model	Train RMSE	Test RMSE	Sparsity Estimate
SS-IG	1.2087±0.0490	1.1947±0.0587	(0.35,0.05)
SV-BNN	1.2897±0.0323	1.2760±0.0363	(0.45,0.35)
HS-BNN	1.2580±0.0305	1.2436±0.0394	(1.00, 1.00)
VBNN	1.1661±0.0335	1.1614±0.0349	NA

6.3 UCI regression datasets

We apply our model to traditional UCI regression datasets (Dua and Graff, 2017) and contrast our performance against SV-BNN, HS-BNN, and VBNN models. We follow the protocol proposed by (Hernandez-Lobato and Adams, 2015) and train a single layer neural network with sigmoid activations. For smaller datasets - *Concrete*, *Wine*, *Power Plant*, *Kin8nm*, we take 50 nodes in the hidden layer, while for larger datasets - *Protein*, *Year*, we take 100 nodes in the hidden layer. We spilt data randomly while maintaining 9:1 train-test ratio in each case and for smaller datasets we repeat this technique 20 times. In *Protein* data we perform 5 repetitions while in *Year* data we use a single random split (more details in the appendix B). For the comparative analysis, we benchmark against SV-BNN, HS-BNN and VBNN. Moreover, VBNN test RMSEs serve as baseline in each dataset. Table 2 summarises our results.

We achieve lower RMSEs compared to SV-BNN and HS-BNN in *Power Plant*, *Kin8nm*, and *Year* datasets and in other cases we achieve comparable RMSE values. In all the datasets, our predictive performance is close to the baseline of VBNN. We provide sparsity estimates (proportion of nodes remaining in the sparse network) in our model and SV-BNN. HS-BNN was not able to achieve sparse structure which is consistent with the results provided in the appendix of (Ghosh et al., 2019). In contrast to HS-BNN, our model sparsifies the model during training without requiring ad-hoc thresholding rule for pruning. Table 2 demonstrates that our model uniformly achieves better sparsity than SV-BNN. In particular, *Concrete* and *Wine* datasets show the high compressive ability of our model over SV-BNN leading to very compact models for inference.

Table 2: Results on UCI regression datasets

Dataset	$n(k_0)$	Test RMSE				Sparsity Estimate	
		SS-IG	SV-BNN	HS-BNN	VBNN	SS-IG	SV-BNN
Concrete	1030 (8)	7.92±0.68	8.22±0.70	5.34±0.53	7.34±0.62	0.42±0.06	0.98±0.02
Wine	1599 (11)	0.66±0.05	0.65±0.05	0.66±0.05	0.64±0.05	0.18±0.05	0.87±0.04
Power Plant	9568 (4)	4.28±0.20	4.32±0.19	4.34±0.18	4.27±0.17	0.18±0.03	0.24±0.03
Kin8nm	8192 (8)	0.09±0.00	0.11±0.01	0.10±0.00	0.09±0.00	0.43±0.04	0.47±0.04
Protein	45730 (9)	4.85±0.05	4.93±0.06	4.59±0.02	4.78±0.06	0.81±0.03	0.93±0.03
Year	515345 (90)	8.68±NA	8.78±NA	9.33±NA	8.67±NA	0.71±NA	0.78±NA

6.4 Image classification: MNIST

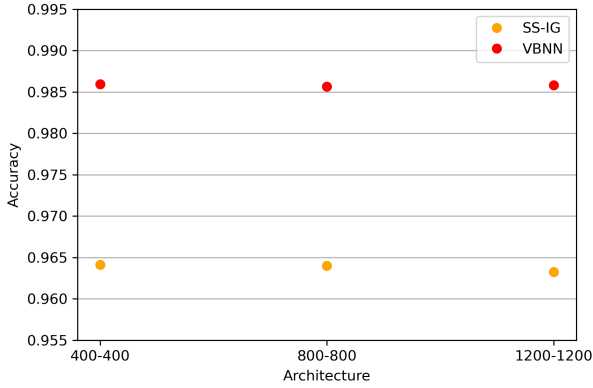
We benchmark empirical performance of our proposed method on MNIST image classification problem. Additional experiment extending our model to convolutional neural network (CNN) setup applied in an

another image classification task presented through Fashion-MNIST dataset is given in appendix B. We compare our model against dense VBNN model which does not sparsify and serves as a baseline.

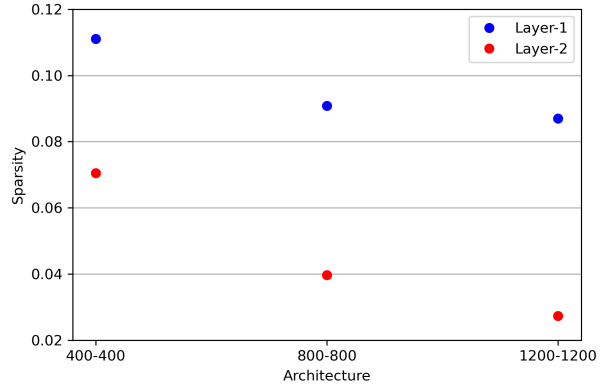
First, we preprocess the images in the MNIST data by dividing the pixel values with 126. We explored 2-hidden layer neural networks with varying widths. We use swish (SiLU) activations (Elfwing et al., 2018; Ramachandran et al., 2017) instead of ReLUs to avoid the dying neuron problem where ReLU neurons become inactive and only output 0 for any input (Lu et al., 2020). Specifically in large scale datasets turning off a node with more than 100 incoming edges adversely impacts the training process of ReLU networks. Smoother activation functions such as sigmoid, tanh, swish etc help alleviate this problem. We choose swish since it gives us the best performance. For our SS-IG model we use 10^{-3} learning rate and minibatch size of 1024 which we choose using extensive hyperparameter search. For VBNN we use the hyperparameter values guided by hyperparameter search and Blundell et al. (2015) where learning rate of 10^{-4} and minibatch size of 128 is finally chosen. We train both the models over 400 epochs with the help of Adam optimizer.

Figure 3 summarizes the results. We have provided results for 3 different architectures which have 400, 800, and 1200 nodes each in their 2-hidden layers. In Figure 3a, we find that across the architectures both SS-IG and VBNN models have similar predictive performance. Further, our method is able to prune off more than 88% of first hidden layer nodes and more than 92% of second hidden layer nodes (Figure 3b) at the expense of 2% accuracy loss due to sparsification compared to the densely connected VBNN. We also observe that as model capacity increases the sparsity percentage per layer decreases. This suggests that, each architecture is trying to reach a sparse network of comparable size.

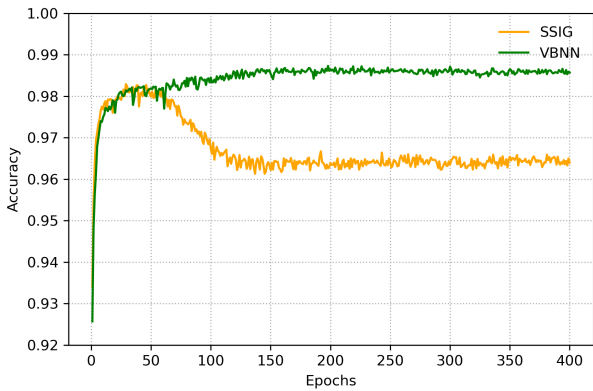
We also provide the plots of predictive accuracy and layer-wise sparsities for 400-400 architecture to further investigate how performance changes as we induce sparsity in our network. In figure 3c, we observe that as we start to learn sparse network our model peaks in predictive performance when most of the nodes are present in the model and it starts to drop as we learn sparser network. The predictive accuracy finally stabilizes after 100 epochs when the sparsity is also converged to a steady state (Figure 3d). We observe similar patterns for accuracy and sparsity trade-offs for rest of the architectures. We can also stop inducing sparsity around 50th epoch where we are left with almost 60% of hidden layer nodes and further train it as a dense model. This could allow for higher predictive performance at the expense of more dense model.



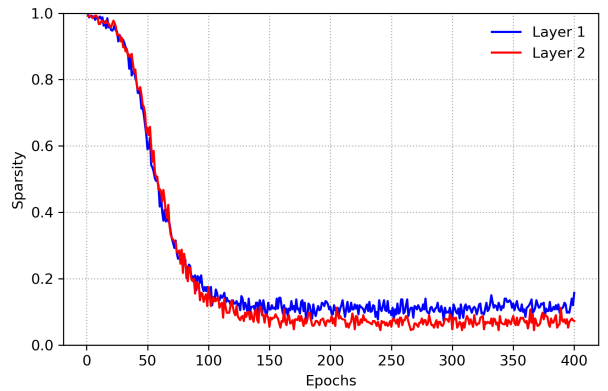
(a) Prediction accuracy per architecture



(b) Layer-wise sparsity per architecture



(c) Prediction accuracy over epochs



(d) Layer-wise sparsity over epochs

Figure 3: MNIST experiment results

7 Conclusion and Discussion

Deep learning has been harnessed by big industrial corporations in recent years to improve their products. However, as deep learning models are pushed into smaller and smaller embedded devices, such as smart cameras recognizing visitors at your front door, designing resource efficient neural networks for real-time, on-device inference is of practical importance. Our work addresses this computational bottleneck by compressing neural networks by inducing structured sparsity during training. The estimation of posterior allows us to quantify uncertainties around the parameter estimates which can be vital in medical diagnostics.

In this paper, we have proposed sparse deep Bayesian neural networks using spike-and-slab priors for optimal node recovery. Our method incorporates layer-wise prior inclusion probabilities and recovers underlying sparse model effectively. Our theoretical developments highlight the conditions required for the posterior consistency of the variational posterior to hold. With layer-wise characterisation of prior inclusion probabilities we show that the proposed sparse BNN approximations can achieve predictive performance comparable to dense networks. Our results relax the constraints of equal number of nodes and uniform bounds on weights thereby achieving optimal node recovery on more generic neural network structure. The closeness of a true function to the topology induced by layer-wise node distribution depends on the degree

of smoothness of the true underlying function. In this work, this has not been well studied and forms a promising direction for future work.

Note, in contrast to previous works, this work assumes a spike-and-slab prior on the entire vector of incoming weights and bias onto a node. The demonstration of its efficacy opens the avenue for exploration of sophisticated group sparsity priors for node selection. Our detailed experiments show the subnetwork selection ability of our method which underscores the notion that deep neural networks can be heavily pruned without losing predictive performance. Additional illustration involving Fashion-MNIST dataset with convolutional neural network indicates the possible generalization of our approach from mere multi layer perceptron to complex deep learning models. Although our method performs model reduction while maintaining predictive power, some further improvements may be obtained by choosing the number of layers in a data-driven fashion and can be a part of future work.

A Proofs of theoretical results

A.1 Definitions

Definition A.1 (Sieve). Consider a sequence of function classes $\mathcal{F}_1 \subseteq \mathcal{F}_2 \subseteq \dots \subseteq \mathcal{F}_n \subseteq \mathcal{F}_{n+1} \subseteq \dots \subseteq \mathcal{F}$, where $\forall f \in \mathcal{F}, \exists f_n \in \mathcal{F}_n$ s.t. $d(f, f_n) \rightarrow 0$ as $n \rightarrow \infty$ where $d(\cdot, \cdot)$ is some pseudo-metric on \mathcal{F} . More precisely, $\cup_{n=1}^{\infty} \mathcal{F}_n$ is dense in \mathcal{F} . \mathcal{F}_n is called a sieve space of \mathcal{F} with respect to the pseudo-metric $d(\cdot, \cdot)$, and the sequence $\{f_n\}$ is called a sieve (Grenander, 1981).

Definition A.2 (Covering number). Let $(V, \|\cdot\|)$ be a normed space, and $\mathcal{F} \subset V$. $\{V_1, \dots, V_N\}$ is an ε -covering of \mathcal{F} if $\mathcal{F} \subset \cup_{i=1}^N B(V_i, \varepsilon)$, or equivalently, $\forall \rho \in \mathcal{F}, \exists i$ such that $\|\rho - V_i\| < \varepsilon$. The covering number of \mathcal{F} denoted by $N(\varepsilon, \mathcal{F}, \|\cdot\|) = \min\{n : \exists \varepsilon\text{-covering over } \mathcal{F} \text{ of size } n\}$ (Pollard, 1991).

A.2 General Lemmas

Lemma A.3. Let g_1 and g_2 be any two density functions. Then

$$E_{g_1}(|\log(g_1/g_2)|) \leq d_{\text{KL}}(g_1, g_2) + 2/e$$

Proof. Refer to Lemma 4 in Lee (2000). □

Lemma A.4. For any $K > 0$, let $\mathbf{a}, \mathbf{a}^0 \in [0, 1]^K$ such that $\sum_{k=1}^K a_k = \sum_{k=1}^K a_k^0 = 1$, then the KL divergence between mixture densities $\sum_{k=1}^K a_k g_k$ and $\sum_{k=1}^K a_k^0 g_k^0$ is bounded as

$$d_{\text{KL}}\left(\sum_{k=1}^K a_k g_k, \sum_{k=1}^K a_k^0 g_k^0\right) \leq d_{\text{KL}}(\mathbf{a}^0, \mathbf{a}) + \sum_{k=1}^K a_k^0 d_{\text{KL}}(g_k^0, g_k)$$

Proof. Refer to Lemma 6.1 in Chérif-Abdellatif and Alquier (2018). □

Lemma A.5.

$$d_{\text{KL}}(\tilde{\pi}^*, \tilde{\pi}(|\mathcal{D})) \leq d_{\text{KL}}(\pi^*, \pi(|\mathcal{D}))$$

Proof. Using Lemma A.4 with $\mathbf{a}^0 = \pi^*(z)$, $\mathbf{a} = \pi(z|\mathcal{D})$, $g^0 = \pi^*(\theta|z)$ and $g = \pi(\theta|z, \mathcal{D})$, we get

$$\begin{aligned} d_{\text{KL}}(\tilde{\pi}^*, \tilde{\pi}(|\mathcal{D})) &= d_{\text{KL}}\left(\sum_z \pi^*(\theta|z) \pi^*(z), \sum_z \pi(\theta|z, \mathcal{D}) \pi(z|\mathcal{D})\right) \\ &\leq d_{\text{KL}}(\pi^*(z), \pi(z|\mathcal{D})) + \sum_z d_{\text{KL}}(\pi^*(\theta|z), \pi(\theta|z, \mathcal{D})) \pi^*(z) \end{aligned}$$

$$= d_{\text{KL}}(\pi^*(\boldsymbol{\theta}, \mathbf{z}), \pi(\boldsymbol{\theta}, \mathbf{z}|\mathcal{D})) = d_{\text{KL}}(\pi^*, \pi(|\mathcal{D}))$$

□

Lemma A.6. For any 1-Lipschitz continuous activation function ψ such that $\psi(x) \leq x \forall x \geq 0$,

$$N(\delta, \mathcal{F}(L, \mathbf{k}, \mathbf{s}, \mathbf{B}), \|\cdot\|_\infty) \leq \sum_{s_L^* \leq s_L} \cdots \sum_{s_0^* \leq s_0} \left[\prod_{l=0}^L \left(\frac{B_l}{\delta B_l / (2(L+1) (\prod_{j=0}^L B_j))} k_{l+1} \right)^{s_l} \right]$$

where N denotes the covering number.

Proof. Given a neural network

$$\eta(\mathbf{x}) = \mathbf{v}_L + \mathbf{W}_L \psi(\mathbf{v}_{L-1} + \mathbf{W}_{L-1} \psi(\mathbf{v}_{L-2} + \mathbf{W}_{L-2} \psi(\cdots \psi(\mathbf{v}_1 + \mathbf{W}_1 \psi(\mathbf{v}_0 + \mathbf{W}_0 \mathbf{x}))))$$

for $l \in \{1, \dots, L\}$, we define $A_l^+ \eta : [0, 1]^p \rightarrow \mathbb{R}^{k_l}$,

$$A_l^+ \eta(\mathbf{x}) = \psi(\mathbf{v}_{l-1} + \mathbf{W}_{l-1} \psi(\mathbf{v}_{l-2} + \mathbf{W}_{l-2} \psi(\cdots \psi(\mathbf{v}_1 + \mathbf{W}_1 \psi(\mathbf{v}_0 + \mathbf{W}_0 \mathbf{x}))))$$

and $A_l^- \eta : \mathbb{R}^{k_{l-1}} \rightarrow \mathbb{R}^{k_{L+1}}$,

$$A_l^- \eta(\mathbf{y}) = \mathbf{v}_L + \mathbf{W}_L \psi(\mathbf{v}_{L-1} + \mathbf{W}_{L-1} \psi(\cdots \psi(\mathbf{v}_l + \mathbf{W}_l \psi(\mathbf{v}_{l-1} + \mathbf{W}_{l-1} \mathbf{y}))))$$

The above framework is also used in the proof of lemma 5 in Schmidt-Hieber (2020). Next, set $A_0^+ \eta(\mathbf{x}) = A_{L+2}^- \eta(\mathbf{x}) = \mathbf{x}$ and further note that for $\eta \in \mathcal{F}(L, \mathbf{k})$, $|A_l^+ \eta(\mathbf{x})|_\infty \leq \prod_{j=0}^{l-1} B_j$ where $\mathbf{k} = (p, k_1, \dots, k_L, k_{L+1})$ and $k_{L+1} = 1$. Next, we derive upper bound on Lipschitz constant of $A_l^- \eta$.

$$|\mathbf{W}_L A_L^+ \eta(\mathbf{x}_1) - \mathbf{W}_L A_L^+ \eta(\mathbf{x}_2)|_\infty = |A_l^- \eta(A_{l-1}^+ \eta(\mathbf{x}_1)) - A_l^- \eta(A_{l-1}^+ \eta(\mathbf{x}_2))|_\infty \quad (14)$$

l.h.s. is bounded above by $\prod_{j=0}^L B_j$ and r.h.s consists of composition of Lipschitz functions $A_l^- \eta$ and $A_{l-1}^+ \eta$ with C_1 and C_2 being corresponding Lipschitz constants. So we can bound r.h.s. by,

$$|A_l^- \eta(A_{l-1}^+ \eta(\mathbf{x}_1)) - A_l^- \eta(A_{l-1}^+ \eta(\mathbf{x}_2))|_\infty \leq C_1 C_2 \|\mathbf{x}_1 - \mathbf{x}_2\|_\infty \quad \forall \mathbf{x}_1, \mathbf{x}_2 \in \mathbb{R}^p$$

If we choose $\mathbf{x}_1 = \mathbf{x} \in [0, 1]^p$ and $\mathbf{x}_2 = \mathbf{0}$ then,

$$|A_l^- \eta(A_{l-1}^+ \eta(\mathbf{x})) - A_l^- \eta(A_{l-1}^+ \eta(\mathbf{0}))|_\infty \leq C_1 C_2 \quad \forall \mathbf{x} \in [0, 1]^p$$

Since C_2 is Lipschitz constant for $A_{l-1}^+ \eta$ and we know that $|A_{l-1}^+ \eta|_\infty \leq \prod_{j=0}^{l-2} B_j$. So we get $C_2 \leq 2 \prod_{j=0}^{l-2} B_j$. We use this in above expression,

$$|A_l^- \eta(A_{l-1}^+ \eta(\mathbf{x})) - A_l^- \eta(A_{l-1}^+ \eta(\mathbf{0}))|_\infty \leq 2C_1 \prod_{j=0}^{l-2} B_j \quad \forall \mathbf{x} \in [0, 1]^p \quad (15)$$

Next we know that l.h.s. of (15) can be bounded above by $2 \prod_{j=0}^L B_j$ because of (14). So we get bound on Lipschitz constant of $A_l^- \eta$,

$$2C_1 \prod_{j=0}^{l-2} B_j \leq 2 \prod_{j=0}^L B_j \implies C_1 \leq \prod_{j=l-1}^L B_j$$

Let $\eta, \eta^* \in \mathcal{F}(L, \mathbf{k}, \mathbf{s}, \mathbf{B})$ be two neural networks with $\overline{\mathbf{W}}_l = (\mathbf{v}_l, \mathbf{W}_l)$ and $\overline{\mathbf{W}}_l^* = (\mathbf{v}_l^*, \mathbf{W}_l^*)$ respectively. Here, we define $\overline{\boldsymbol{\delta}}_l$ using the L_1 norms of the rows of $\overline{\mathbf{D}}_l = \overline{\mathbf{W}}_l - \overline{\mathbf{W}}_l^*$ as follows

$$\overline{\mathbf{D}}_l = (\overline{\mathbf{d}}_{l1}^\top, \dots, \overline{\mathbf{d}}_{lk_{l+1}}^\top)^\top \quad \overline{\boldsymbol{\delta}}_l = (\|\overline{\mathbf{d}}_{l1}\|_1, \dots, \|\overline{\mathbf{d}}_{lk_{l+1}}\|_1)$$

We choose η, η^* such that $\|\overline{\boldsymbol{\delta}}_l\|_\infty \leq \zeta B_l$. This also means that all parameters in each layer of these two networks are at most ζB_l distance away from each other. Then, we can bound the absolute difference between these two neural networks by,

$$\begin{aligned} & |\eta(\mathbf{x}) - \eta^*(\mathbf{x})| \\ & \leq \sum_{l=1}^{L+1} |A_{l+1}^- \eta(\psi(\mathbf{v}_{l-1} + \mathbf{W}_{l-1} A_{l-1}^+ \eta^*(\mathbf{x}))) - A_{l+1}^- \eta(\psi(\mathbf{v}_{l-1}^* + \mathbf{W}_{l-1}^* A_{l-1}^+ \eta^*(\mathbf{x})))| \\ & \leq \sum_{l=1}^{L+1} \left(\prod_{j=l}^L B_j \right) \|\psi(\mathbf{v}_{l-1} + \mathbf{W}_{l-1} A_{l-1}^+ \eta^*(\mathbf{x})) - \psi(\mathbf{v}_{l-1}^* + \mathbf{W}_{l-1}^* A_{l-1}^+ \eta^*(\mathbf{x}))\|_\infty \\ & \leq \sum_{l=1}^{L+1} \left(\prod_{j=l}^L B_j \right) \|\mathbf{v}_{l-1} - \mathbf{v}_{l-1}^* + (\mathbf{W}_{l-1} - \mathbf{W}_{l-1}^*) A_{l-1}^+ \eta^*(\mathbf{x})\|_\infty \\ & \leq \sum_{l=1}^{L+1} \left(\prod_{j=l}^L B_j \right) \|\overline{\boldsymbol{\delta}}_{l-1}\|_\infty \|A_{l-1}^+ \eta^*(\mathbf{x})\|_\infty \\ & \leq \sum_{l=1}^{L+1} \left(\prod_{j=l}^L B_j \right) \zeta B_{l-1} \prod_{j=0}^{l-2} B_j = \zeta(L+1) \left(\prod_{j=0}^L B_j \right) \end{aligned} \quad (16)$$

Recall that we have at most k_l number of nodes in each layer and there are $\binom{k_{l+1}}{s_l} \leq k_{l+1}^{s_l}$ combinations of nodes to choose s_l active nodes in the given layer. Since supremum norm of L_1 norms of the rows of $\overline{\mathbf{W}}_l$ is bounded above by B_l in our family of neural networks $\mathcal{F}(L, \mathbf{k}, \mathbf{s}, \mathbf{B})$ so we can discretize these L_1 norms with grid size $\delta B_l / (2(L+1)(\prod_{j=0}^L B_j))$ and obtain upper bound on covering number as follows

$$\begin{aligned} N(\delta, \mathcal{F}(L, \mathbf{k}, \mathbf{s}, \mathbf{B}), \|\cdot\|_\infty) & \leq \sum_{s_L^* \leq s_L} \cdots \sum_{s_0^* \leq s_0} \left[\prod_{l=0}^L \left(\frac{B_l}{\delta B_l / (2(L+1)(\prod_{j=0}^L B_j))} k_{l+1} \right)^{s_l} \right] \\ & \leq \prod_{l=0}^L \left(2\delta^{-1}(L+1) \left(\prod_{j=0}^L B_j \right) k_{l+1} \right)^{(s_l+1)} \end{aligned} \quad (17)$$

□

Lemma A.7. Let $\boldsymbol{\theta}^* = \arg \min_{\boldsymbol{\theta} \in \mathcal{F}(L, \mathbf{k}, \mathbf{s}, \mathbf{B})} \|\eta_{\boldsymbol{\theta}} - \eta_0\|_\infty^2$ and $\widetilde{\mathbf{W}}_l = \sup_i \|\overline{\mathbf{w}}_{li} - \overline{\mathbf{w}}_{li}^*\|_1$, then for any density $q = \prod_{j=0}^L q(\theta_j)$,

$$\begin{aligned} \int \|\eta_{\boldsymbol{\theta}} - \eta_{\boldsymbol{\theta}^*}\|_2^2 q(\boldsymbol{\theta}) d\boldsymbol{\theta} & \leq \sum_{j=0}^L c_{j-1}^2 \int \widetilde{\mathbf{W}}_j^2 q_j(\theta_j) d\theta_j \prod_{m=j+1}^L \int (\widetilde{\mathbf{W}}_m + B_m)^2 q(\boldsymbol{\theta}) d\boldsymbol{\theta} \\ & + 2 \sum_{j=0}^L \sum_{j'=0}^{j-1} c_{j-1} c_{j'-1} \int \widetilde{\mathbf{W}}_j (\widetilde{\mathbf{W}}_j + B_j) q_j(\theta_j) d\theta_j \prod_{m=j+1}^L \int (\widetilde{\mathbf{W}}_m + B_m)^2 q(\boldsymbol{\theta}) d\boldsymbol{\theta} \end{aligned}$$

$$\times \int \widetilde{W}_{j'} q_{j'}(\theta_{j'}) d\theta_{j'} \prod_{m=j'+1}^{j-1} \int (\widetilde{W}_m + B_m) q(\boldsymbol{\theta}) d\boldsymbol{\theta} \quad (18)$$

where $c_{j-1} \leq \prod_{m=0}^{j-1} B_m$.

Proof. Let $\eta_{\boldsymbol{\theta}}^l$ be the partial networks defined as

$$\begin{cases} \eta_{\boldsymbol{\theta}}^0(\mathbf{x}) := \psi(\mathbf{W}_0 \mathbf{x} + \mathbf{v}_0), \\ \eta_{\boldsymbol{\theta}}^l(\mathbf{x}) := \psi(\mathbf{W}_l \eta_{\boldsymbol{\theta}}^{l-1}(\mathbf{x}) + \mathbf{v}_l), \\ \eta_{\boldsymbol{\theta}}^L(\mathbf{x}) := \mathbf{W}_L \eta_{\boldsymbol{\theta}}^{L-1}(\mathbf{x}) + \mathbf{v}_L. \end{cases}$$

Similar to the proof of theorem 2 in Chérif-Abdellatif (2020), define

$$\varphi_l(\boldsymbol{\theta}) = \sup_{\mathbf{x} \in [0,1]^p} \sup_{1 \leq i \leq k_{l+1}} |\eta_{\boldsymbol{\theta}}^l(\mathbf{x})_i - \eta_{\boldsymbol{\theta}^*}^l(\mathbf{x})_i|.$$

We next show by induction

$$\varphi_l(\boldsymbol{\theta}) \leq \sum_{j=0}^l \widetilde{W}_j c_{j-1} R_{j+1}^l$$

where we define $c_l = \max(\sup_{\mathbf{x} \in [0,1]^p} \sup_{1 \leq i \leq k_{l+1}} |\eta_{\boldsymbol{\theta}^*}^l(\mathbf{x})_i|, 1)$, $c_0 = 1$, $R_{j+1}^l = \prod_{m=j+1}^l (\widetilde{W}_m + B_m)$.

Claim: $c_l \leq B_l c_{l-1}$. Note

$$\begin{aligned} c_l &\leq \sup_{\mathbf{x} \in [0,1]^p} \sup_{1 \leq i \leq k_{l+1}} (|\mathbf{w}_{li}^{*\top} \eta_{\boldsymbol{\theta}^*}^{l-1}(\mathbf{x})| + |v_{li}|) \\ &\leq \sup_{\mathbf{x} \in [0,1]^p} \sup_{1 \leq i \leq k_{l+1}} \left(\sum_{j=1}^{k_l} |w_{lij}^*| |\eta_{\boldsymbol{\theta}^*}^{l-1}(\mathbf{x})_j| + |v_{li}| \right) \\ &\leq \sup_{1 \leq i \leq k_{l+1}} \left(c_{l-1} \sum_{j=1}^{k_l} |w_{lij}^*| + c_{l-1} |v_{li}| \right) \\ &\leq c_{l-1} \sup_{1 \leq i \leq k_{l+1}} \|\overline{\mathbf{w}}_{li}^*\|_1 = B_l c_{l-1} \end{aligned}$$

where the above result holds since $\sup_i \|\overline{\mathbf{w}}_{li}^*\|_1 \leq B_l$. Next,

$$\begin{aligned} \varphi_l(\boldsymbol{\theta}) &\leq \sup_{\mathbf{x} \in [0,1]^p} \sup_{1 \leq i \leq k_{l+1}} \left(\sum_{j=1}^{k_l} |w_{lij} \eta_{\boldsymbol{\theta}}^{l-1}(\mathbf{x})_j - w_{lij}^* \eta_{\boldsymbol{\theta}^*}^{l-1}(\mathbf{x})_j| + |v_{li} - v_{li}^*| \right) \\ &\leq \sup_{\mathbf{x} \in [0,1]^p} \sup_{1 \leq i \leq k_{l+1}} \left(\sum_{j=1}^{k_l} |w_{lij} \eta_{\boldsymbol{\theta}}^{l-1}(\mathbf{x})_j - w_{lij}^* \eta_{\boldsymbol{\theta}}^{l-1}(\mathbf{x})_j| \right. \\ &\quad \left. + |w_{lij}^* \eta_{\boldsymbol{\theta}}^{l-1}(\mathbf{x})_j - w_{lij}^* \eta_{\boldsymbol{\theta}^*}^{l-1}(\mathbf{x})_j| + |v_{li} - v_{li}^*| \right) \\ &\leq \sup_{\mathbf{x} \in [0,1]^p} \sup_{1 \leq i \leq k_{l+1}} \left(\sum_{j=1}^{k_l} |w_{lij} - w_{lij}^*| |\eta_{\boldsymbol{\theta}}^{l-1}(\mathbf{x})_j| \right. \\ &\quad \left. + \sum_{j=1}^{k_l} |w_{lij}^*| |\eta_{\boldsymbol{\theta}}^{l-1}(\mathbf{x})_j - \eta_{\boldsymbol{\theta}^*}^{l-1}(\mathbf{x})_j| + |v_{li} - v_{li}^*| \right) \end{aligned}$$

$$\begin{aligned}
&\leq \sup_{\mathbf{x} \in [0,1]^p} \sup_{1 \leq i \leq k_{l+1}} \left(\sum_{j=1}^{k_l} |w_{lij} - w_{lij}^*| |\eta_{\boldsymbol{\theta}}^{l-1}(\mathbf{x})_j - \eta_{\boldsymbol{\theta}^*}^{l-1}(\mathbf{x})_j| \right. \\
&\quad \left. + \sum_{j=1}^{k_l} |w_{lij} - w_{lij}^*| |\eta_{\boldsymbol{\theta}^*}^{l-1}(\mathbf{x})_j| + |v_{li} - v_{li}^*| \right) + \varphi_{l-1}(\boldsymbol{\theta}) B_l \\
&\leq \widetilde{W}_l (\varphi_{l-1}(\boldsymbol{\theta}) + c_{l-1}) + \varphi_{l-1}(\boldsymbol{\theta}) B_l = \varphi_{l-1}(\boldsymbol{\theta}) (\widetilde{W}_l + B_l) + c_{l-1} \widetilde{W}_l
\end{aligned}$$

Now applying recursion we get

$$\begin{aligned}
\varphi_l(\boldsymbol{\theta}) &\leq (\varphi_{l-2}(\boldsymbol{\theta}) (\widetilde{W}_{l-1} + B_{l-1}) + c_{l-2} \widetilde{W}_{l-1}) (\widetilde{W}_l + B_l) + c_{l-1} \widetilde{W}_l \\
&= \varphi_{l-2}(\boldsymbol{\theta}) (\widetilde{W}_l + B_l) (\widetilde{W}_{l-1} + B_{l-1}) + c_{l-2} \widetilde{W}_{l-1} (\widetilde{W}_l + B_l) + c_{l-1} \widetilde{W}_l
\end{aligned}$$

Repeating this we get

$$\begin{aligned}
\varphi_l(\boldsymbol{\theta}) &\leq \varphi_0(\boldsymbol{\theta}) \prod_{j=1}^l (\widetilde{W}_j + B_j) + \sum_{j=1}^l c_{j-1} \widetilde{W}_j \prod_{u=j+1}^l (\widetilde{W}_j + B_j) \\
&= \widetilde{W}_0 \prod_{j=1}^l (\widetilde{W}_j + B_j) + \sum_{j=1}^l B_1 \cdots B_{j-1} \widetilde{W}_j \prod_{u=j+1}^l (\widetilde{W}_j + B_j) \\
&= \sum_{j=0}^l B_1 \cdots B_{j-1} \widetilde{W}_j \prod_{u=j+1}^l (\widetilde{W}_j + B_j) = \sum_{j=0}^l \widetilde{W}_j c_{j-1} R_{j+1}^l
\end{aligned}$$

$$\begin{aligned}
&\int \|\eta_{\boldsymbol{\theta}} - \eta_{\boldsymbol{\theta}^*}\|_2^2 q(\boldsymbol{\theta}) d\boldsymbol{\theta} \leq \int \|\eta_{\boldsymbol{\theta}} - \eta_{\boldsymbol{\theta}^*}\|_\infty^2 q(\boldsymbol{\theta}) d\boldsymbol{\theta} = \int \varphi_L^2(\boldsymbol{\theta}) q(\boldsymbol{\theta}) d\boldsymbol{\theta} \\
&= \int \left(\sum_{j=0}^L \widetilde{W}_j c_{j-1} R_{j+1}^L \right)^2 q(\boldsymbol{\theta}) d\boldsymbol{\theta} \\
&= \sum_{j=0}^L c_{j-1}^2 \int \widetilde{W}_j^2 (R_{j+1}^L)^2 q(\boldsymbol{\theta}) d\boldsymbol{\theta} + 2 \sum_{j=0}^L \sum_{j'=0}^{j-1} c_{j-1} c_{j'-1} \int \widetilde{W}_j \widetilde{W}_{j'} R_{j+1}^L R_{j'+1}^L q(\boldsymbol{\theta}) d\boldsymbol{\theta} \\
&= \sum_{j=0}^L c_{j-1}^2 \int \widetilde{W}_j^2 \left(\prod_{m=j+1}^L (\widetilde{W}_m + B_m) \right)^2 q(\boldsymbol{\theta}) d\boldsymbol{\theta} \\
&\quad + 2 \sum_{j=0}^L \sum_{j'=0}^{j-1} c_{j-1} c_{j'-1} \int \widetilde{W}_j \widetilde{W}_{j'} \prod_{m=j+1}^L (\widetilde{W}_m + B_m) \prod_{m=j'+1}^L (\widetilde{W}_m + B_m) q(\boldsymbol{\theta}) d\boldsymbol{\theta}
\end{aligned}$$

The proof follows by noting $q(\boldsymbol{\theta}) = \prod_{j=0}^L q(\theta_j)$. □

Lemma A.8. *Suppose Lemma 4.1 and Lemma 4.2 in the main paper hold, with dominating probability*

$$\log \int_{\mathcal{H}_{\epsilon_n}} \frac{P_{\boldsymbol{\theta}}^n}{P_0^n} \pi(\boldsymbol{\theta}) d\boldsymbol{\theta} \leq -\frac{C n \epsilon_n^2}{\sum u_l}$$

Proof. Let $\mathcal{F}_n = \mathcal{F}(L, \mathbf{k}, \mathbf{s}^\circ, \mathbf{B}^\circ)$, $s_l^\circ + 1 = n \epsilon_n^2 / \sum_{j=0}^L u_j$, $\log B_l^\circ = n \epsilon_n^2 / ((L+1) \sum_{j=0}^L (s_j^\circ + 1))$ and $\mathcal{H}_{\epsilon_n} =$

$\{\boldsymbol{\theta} : d_{\text{H}}(P_0, P_{\boldsymbol{\theta}}) < \epsilon_n\}$ is the Hellinger neighborhood of size ϵ_n

$$\begin{aligned} \int_{\mathcal{H}_{\epsilon_n}^c} \frac{P_{\boldsymbol{\theta}}^n}{P_0^n} \tilde{\pi}(\boldsymbol{\theta}) d\boldsymbol{\theta} &\leq \int_{\mathcal{H}_{\epsilon_n}^c \cap \mathcal{F}_n} \frac{P_{\boldsymbol{\theta}}^n}{P_0^n} \tilde{\pi}(\boldsymbol{\theta}) d\boldsymbol{\theta} + \int_{\mathcal{F}_n^c} \frac{P_{\boldsymbol{\theta}}^n}{P_0^n} \tilde{\pi}(\boldsymbol{\theta}) d\boldsymbol{\theta} \\ &\leq \int_{\mathcal{H}_{\epsilon_n}^c \cap \mathcal{F}_n} \frac{P_{\boldsymbol{\theta}}^n}{P_0^n} \tilde{\pi}(\boldsymbol{\theta}) d\boldsymbol{\theta} + \exp\left(-\frac{(C_0/2)n\epsilon_n^2}{\sum u_l}\right) \end{aligned}$$

where the last inequality follows from Lemma 4.2 because by Markov's inequality

$$\begin{aligned} \mathbb{P}_{P_0^n} \left(\int_{\mathcal{F}_n^c} \frac{P_{\boldsymbol{\theta}}^n}{P_0^n} \tilde{\pi}(\boldsymbol{\theta}) d\boldsymbol{\theta} > \exp\left(-\frac{(C_0/2)n\epsilon_n^2}{\sum u_l}\right) \right) &\leq \exp\left(\frac{(C_0/2)n\epsilon_n^2}{\sum u_l}\right) \mathbb{E}_{P_0^n} \left(\int_{\mathcal{F}_n^c} \frac{P_{\boldsymbol{\theta}}^n}{P_0^n} \tilde{\pi}(\boldsymbol{\theta}) d\boldsymbol{\theta} \right) \\ &\leq \exp\left(\frac{(C_0/2)n\epsilon_n^2}{\sum u_l}\right) \tilde{\Pi}(\mathcal{F}_n^c) = \exp\left(-\frac{(C_0/2)n\epsilon_n^2}{\sum u_l}\right) \rightarrow 0 \end{aligned}$$

Further,

$$\int_{\mathcal{H}_{\epsilon_n}^c \cap \mathcal{F}_n} \frac{P_{\boldsymbol{\theta}}^n}{P_0^n} \tilde{\pi}(\boldsymbol{\theta}) d\boldsymbol{\theta} \leq \underbrace{\int_{\mathcal{H}_{\epsilon_n}^c \cap \mathcal{F}_n} \phi \frac{P_{\boldsymbol{\theta}}^n}{P_0^n} \tilde{\pi}(\boldsymbol{\theta}) d\boldsymbol{\theta}}_{T_1} + \underbrace{\int_{\mathcal{H}_{\epsilon_n}^c \cap \mathcal{F}_n} (1-\phi) \frac{P_{\boldsymbol{\theta}}^n}{P_0^n} \tilde{\pi}(\boldsymbol{\theta}) d\boldsymbol{\theta}}_{T_2}$$

Next, borrowing steps from proof of theorem 3.1 in Pati et al. (2018), we have $\mathbb{E}_{P_0^n}(\phi) \leq \exp(-C_1 n \epsilon_n^2)$, thus for any $C'_1 < C_1$, $\phi \leq \exp(-C'_1 n \epsilon_n^2)$ with probability at least $1 - \exp(-(C_1 - C'_1) n \epsilon_n^2)$. Thus,

$$T_1 \leq \exp(-C'_1 n \epsilon_n^2) T_1 + T_2$$

which implies with dominating probability $T_1 \leq T_2$. Thus, it only remains to show $T_2 \leq \exp(-C'_2 (n \epsilon_n^2) / (\sum u_l))$ for some $C'_2 > 0$. This is true since

$$\begin{aligned} \mathbb{P}_{P_0^n}(T_2 > e^{-\frac{C_2 n \epsilon_n^2}{\sum u_l}}) &\leq e^{C_2 \frac{n \epsilon_n^2}{\sum u_l}} \mathbb{E}_{P_0^n}(T_2) \leq e^{\frac{C_2 n \epsilon_n^2}{\sum u_l}} \int_{\mathcal{H}_{\epsilon_n}^c \cap \mathcal{F}_n} \mathbb{E}_{P_{\boldsymbol{\theta}}}(1-\phi) \tilde{\pi}(\boldsymbol{\theta}) d\boldsymbol{\theta} \\ &\leq e^{\frac{C_2 n \epsilon_n^2}{\sum u_l}} \int_{\mathcal{H}_{\epsilon_n}^c \cap \mathcal{F}_n} e^{-C_2 n d_{\text{H}}^2(P_0, P_{\boldsymbol{\theta}})} \tilde{\pi}(\boldsymbol{\theta}) d\boldsymbol{\theta} \\ &\leq e^{\frac{C_2 n \epsilon_n^2}{\sum u_l}} e^{-C_2 n \epsilon_n^2} \int_{\mathcal{H}_{\epsilon_n}^c \cap \mathcal{F}_n} \tilde{\pi}(\boldsymbol{\theta}) d\boldsymbol{\theta} \leq \exp(-C'_2 n \epsilon_n^2 / \sum u_l) \end{aligned}$$

Therefore, for sufficiently large n and $C = \min(C_0/2, C'_2)/2$

$$\int_{\mathcal{H}_{\epsilon_n}^c} \frac{P_{\boldsymbol{\theta}}^n}{P_0^n} \tilde{\pi}(\boldsymbol{\theta}) d\boldsymbol{\theta} \leq 2 \exp(-C'_2 n \epsilon_n^2 / \sum u_l) + \exp(-(C_0/2) n \epsilon_n^2 / \sum u_l) \leq \exp(-C n \epsilon_n^2 / \sum u_l)$$

□

Lemma A.9. *Suppose Lemma 4.3 part 1. in the main paper holds, then for any $M_n \rightarrow \infty$, with dominating probability,*

$$\log \int \frac{P_0^n}{P_{\boldsymbol{\theta}}^n} \tilde{\pi}(\boldsymbol{\theta}) d\boldsymbol{\theta} \leq n M_n (\sum r_l + \xi)$$

Proof. By Markov's inequality,

$$\begin{aligned} \mathbb{P}_{P_0^n} \left(\log \int \frac{P_0^n}{P_\theta^n} \tilde{\pi}(\boldsymbol{\theta}) \geq nM_n(\sum r_l + \xi) \right) &\leq \frac{1}{nM_n(\sum r_l + \xi)} \mathbb{E}_{P_0^n} \left| \log \int \frac{P_\theta^n}{P_0^n} \tilde{\pi}(\boldsymbol{\theta}) d\boldsymbol{\theta} \right| \\ &= \frac{1}{nM_n(\sum r_l + \xi)} \int \left| \log \int \frac{P_\theta^n}{P_0^n} \tilde{\pi}(\boldsymbol{\theta}) d\boldsymbol{\theta} \right| P_0^n d\mu \\ &\leq \frac{1}{nM_n(\sum r_l + \xi)} \left(d_{\text{KL}}(P_0^n, L^*) + \frac{2}{e} \right) \end{aligned}$$

where $L^* = \int P_\theta^n \tilde{\pi}(\boldsymbol{\theta}) d\boldsymbol{\theta}$ and the last inequality follows from Lemma A.3.

$$\begin{aligned} d_{\text{KL}}(P_0^n, L^*) &= \mathbb{E}_{P_0^n} \left(\log \frac{P_0^n}{\int P_\theta^n \tilde{\pi}(\boldsymbol{\theta}) d\boldsymbol{\theta}} \right) \leq \mathbb{E}_{P_0^n} \left(\log \frac{P_0^n}{\int_{\mathcal{N}_{\sum r_l + \xi}} P_\theta^n \tilde{\pi}(\boldsymbol{\theta}) d\boldsymbol{\theta}} \right) \\ &\leq \int_{\mathcal{N}_{\sum r_l + \xi}} \tilde{\pi}(\boldsymbol{\theta}) d\boldsymbol{\theta} + \int_{\mathcal{N}_{\sum r_l + \xi}} d_{\text{KL}}(P_0^n, P_\theta^n) \tilde{\pi}(\boldsymbol{\theta}) d\boldsymbol{\theta} \quad \text{Jensen's inequality} \\ &\leq -\log e^{-nC(\sum r_l + \xi)} + n(\sum r_l + \xi) = n(C+1)(\sum r_l + \xi) \end{aligned}$$

where the last inequality follows from Lemma 4.3 part 1. in the main paper. The proof follows by noting $C/M_n \rightarrow 0$. \square

Lemma A.10. *Suppose Lemma 4.3 part 2. in the main paper holds, then for any $M_n \rightarrow \infty$, with dominating probability,*

$$d_{\text{KL}}(q, \pi) + \sum_{\mathbf{z}} \int \log \frac{P_0^n}{P_\theta^n} q(\boldsymbol{\theta}, \mathbf{z}) d\boldsymbol{\theta} \leq nM_n(\sum r_l + \xi)$$

Proof.

By Markov's inequality we have

$$\begin{aligned} &\mathbb{P}_{P_0^n} \left(d_{\text{KL}}(q, \pi) + \sum_{\mathbf{z}} \int q(\boldsymbol{\theta}, \mathbf{z}) \log \frac{P_0^n}{P_\theta^n} d\boldsymbol{\theta} > nM_n(\sum r_l + \xi) \right) \\ &\leq \frac{1}{nM_n(\sum r_l + \xi)} \left(d_{\text{KL}}(q, \pi) + \mathbb{E}_{P_0^n} \left| \sum_{\mathbf{z}} \int q(\boldsymbol{\theta}, \mathbf{z}) \log \frac{P_0^n}{P_\theta^n} d\boldsymbol{\theta} \right| \right) \\ &\leq \frac{1}{nM_n(\sum r_l + \xi)} \left(d_{\text{KL}}(q, \pi) + \mathbb{E}_{P_0^n} \left(\sum_{\mathbf{z}} \int q(\boldsymbol{\theta}, \mathbf{z}) \left| \log \frac{P_\theta^n}{P_0^n} \right| d\boldsymbol{\theta} \right) \right) \\ &= \frac{1}{nM_n(\sum r_l + \xi)} \left(d_{\text{KL}}(q, \pi) + \sum_{\mathbf{z}} \int q(\boldsymbol{\theta}, \mathbf{z}) \int \left| \log \frac{P_\theta^n}{P_0^n} \right| P_0^n d\mu d\boldsymbol{\theta} \right) \end{aligned}$$

By Lemma A.3, we get

$$\begin{aligned} &\leq \frac{1}{nM_n(\sum r_l + \xi)} \left(d_{\text{KL}}(q, \pi) + \sum_{\mathbf{z}} \int q(\boldsymbol{\theta}, \mathbf{z}) \left(d_{\text{KL}}(P_0^n, P_\theta^n) + \frac{2}{e} \right) d\boldsymbol{\theta} \right) \\ &= \frac{1}{nM_n(\sum r_l + \xi)} \left(d_{\text{KL}}(q, \pi) + n \sum_{\mathbf{z}} \int q(\boldsymbol{\theta}, \mathbf{z}) d_{\text{KL}}(P_0, P_\theta) d\boldsymbol{\theta} + \frac{2}{e} \right) \\ &= \frac{C}{nM_n(\sum r_l + \xi)} \left(n(\sum r_l + \xi) + (2/e) \right) \rightarrow 0 \end{aligned}$$

where the last line in the above holds due to Lemma 4.3 part 2. in the main paper. \square

A.3 Proof of Lemmas and Corollary in the main paper

Proof of Lemma 4.1

Take $s_l^\circ + 1 = (n\epsilon_n^2)/(\sum_{j=0}^L u_j)$ and $\log B_l^\circ = (n\epsilon_n^2)/((L+1)\sum_{j=0}^L (s_j^\circ + 1))$.

We know from Lemma 2 of Ghosal and van der Vaart (2007) that, there exists a function $\varphi \in [0, 1]$, such that

$$\begin{aligned}\mathbb{E}_{P_0}(\varphi) &\leq \exp\{-nd_{\mathbb{H}}^2(P_{\theta_1}, P_0)/2\} \\ \mathbb{E}_{P_{\theta}}(1 - \varphi) &\leq \exp\{-nd_{\mathbb{H}}^2(P_{\theta_1}, P_0)/2\}\end{aligned}$$

for all $P_{\theta} \in \mathcal{F}(L, \mathbf{k}, \mathbf{s}^\circ, \mathbf{B}^\circ)$ satisfying $d_{\mathbb{H}}(P_{\theta}, P_{\theta_1}) \leq d_{\mathbb{H}}(P_0, P_{\theta_1})/18$.

Let $H = N(\epsilon_n/19, \mathcal{F}(L, \mathbf{k}, \mathbf{s}^\circ, \mathbf{B}^\circ), d_{\mathbb{H}}(\cdot, \cdot))$ denote the covering number of $\mathcal{F}(L, \mathbf{k}, \mathbf{s}^\circ, \mathbf{B}^\circ)$, i.e., there exist H Hellinger balls of radius $\epsilon_n/19$, that entirely cover $\mathcal{F}(L, \mathbf{k}, \mathbf{s}^\circ, \mathbf{B}^\circ)$. For any $\theta \in \mathcal{F}(L, \mathbf{k}, \mathbf{s}^\circ, \mathbf{B}^\circ)$ w.l.o.g we assume P_{θ} belongs to the Hellinger ball centered at P_{θ_h} and if $d_{\mathbb{H}}(P_{\theta}, P_0) > \epsilon_n$, then we must have that $d_{\mathbb{H}}(P_0, P_{\theta_h}) > (18/19)\epsilon_n$ and there exists a testing function φ_h , such that

$$\begin{aligned}\mathbb{E}_{P_0}(\varphi_h) &\leq \exp\{-nd_{\mathbb{H}}^2(P_{\theta_h}, P_0)/2\} \\ &\leq \exp\{-((18^2/19^2)/2)n\epsilon_n^2\} \\ \mathbb{E}_{P_{\theta}}(1 - \varphi_h) &\leq \exp\{-nd_{\mathbb{H}}^2(P_{\theta_h}, P_0)/2\} \\ &\leq \exp\{-n(d_{\mathbb{H}}(P_0, P_{\theta}) - \epsilon_n/19)^2/2\} \\ &\leq \exp\{-((18^2/19^2)/2)nd_{\mathbb{H}}^2(P_0, P_{\theta})\}.\end{aligned}$$

Next we define $\phi = \max_{h=1, \dots, H} \varphi_h$. Then we must have

$$\begin{aligned}\mathbb{E}_{P_0}(\phi) &\leq \sum_h \mathbb{E}_{P_0}(\varphi_h) \leq H \exp\{-((18^2/19^2)/2)n\epsilon_n^2\} \\ &\leq \exp\{-((18^2/19^2)/2)n\epsilon_n^2 - \log H\}\end{aligned}$$

Using Lemma A.6 with $\mathbf{s} = \mathbf{s}^\circ$ and $\mathbf{B} = \mathbf{B}^\circ$, we get

$$\begin{aligned}\log H &= \log N(\epsilon_n/19, \mathcal{F}(L, \mathbf{k}, \mathbf{s}^\circ, \mathbf{B}^\circ), d_{\mathbb{H}}(\cdot, \cdot)) \\ &\leq \log N(\sqrt{8}\sigma_e^2\epsilon_n/19, \mathcal{F}(L, \mathbf{k}, \mathbf{s}^\circ, \mathbf{B}^\circ), \|\cdot\|_{\infty}) \\ &\leq \log \left[\prod_{l=0}^L \left(\frac{38}{\sqrt{8}\sigma_e^2\epsilon_n} (L+1) \left(\prod_{j=0}^L B_j^\circ \right) k_{l+1} \right)^{(s_l^\circ + 1)} \right] \\ &= \sum_{l=0}^L (s_l^\circ + 1) \log \left(\frac{38}{\sqrt{8}\sigma_e^2\epsilon_n} (L+1) \left(\prod_{j=0}^L B_j^\circ \right) k_{l+1} \right) \\ &\leq C \left[\sum_{l=0}^L (s_l^\circ + 1) \left(\log \frac{1}{\epsilon_n} + \log(L+1) + \sum_{j=0}^L \log B_j^\circ + \log k_{l+1} \right) \right] \\ &\leq C \sum_{l=0}^L (s_l^\circ + 1) (\log n + \log(L+1) + \sum_{j=0}^L \log B_j^\circ + \log k_{l+1})\end{aligned}$$

$$\leq C \sum_{l=0}^L (s_l^\circ + 1)(\log n + \log(L+1) + \sum_{j=0}^L \log B_j^\circ + \log k_{l+1} + \log(k_l + 1)) \leq C n \epsilon_n^2$$

where, C in each step is different which tends to absorb the extra constants in it. First inequality holds due to the following

$$d_{\mathbb{H}}^2(P_\theta, P_0) \leq 1 - \exp\left\{-\frac{1}{8\sigma_\epsilon^2} \|\eta_0 - \eta_\theta\|_\infty^2\right\}$$

and $\epsilon_n = o(1)$, the second inequality is due to (17), and fourth inequality is due to $s_l^\circ \log(1/\epsilon_n) \asymp s_l^\circ \log n$. Therefore,

$$\mathbb{E}_{P_0}(\phi) \leq \sum_h \mathbb{E}_{P_0}(\varphi_h) = \exp\{-C_1 n \epsilon_n^2\}$$

for some $C_1 = (18^2/19^2)/2 - 1/4$. On the other hand, for any θ , such that $d_{\mathbb{H}}(P_\theta, P_0) \geq \epsilon_n$, say P_θ belongs to the h th Hellinger ball, then we have

$$\mathbb{E}_{P_\theta}(1 - \phi) \leq \mathbb{E}_{P_\theta}(1 - \varphi_h) \leq \exp\{-C_2 n d_{\mathbb{H}}^2(P_0, P_\theta)\}$$

where $C_2 = (18^2/19^2)/2$. This concludes the proof. \square

Proof of Lemma 4.2

$$\text{Assumption : } s_l^\circ + 1 = (n\epsilon_n^2)/\left(\sum_{j=0}^L u_j\right), \lambda_l k_{l+1}/s_l^\circ \rightarrow 0, \sum u_l \log L = o(n\epsilon_n^2) \quad (19)$$

$$\begin{aligned} \tilde{\Pi}(\mathcal{F}(L, \mathbf{k}, \mathbf{s}^\circ, \mathbf{B}^\circ)^c) &\leq \tilde{\Pi}\left(\bigcup_{l=0}^L \{\|\tilde{\mathbf{w}}_l\|_0 > s_l^\circ\}\right) + \tilde{\Pi}\left(\bigcup_{l=0}^L \{\|\tilde{\mathbf{w}}_l\|_\infty > B_l^\circ\}\right) \\ &\leq \sum_{l=0}^L \tilde{\Pi}(\|\tilde{\mathbf{w}}_l\|_0 > s_l^\circ) + \sum_{l=0}^L \tilde{\Pi}(\|\tilde{\mathbf{w}}_l\|_\infty > B_l^\circ) \\ &= \sum_{l=0}^L \sum_{\mathbf{z}} \Pi(\|\tilde{\mathbf{w}}_l\|_0 > s_l^\circ | \mathbf{z}) \pi(\mathbf{z}) + \sum_{l=0}^L \sum_{\mathbf{z}} \Pi(\|\tilde{\mathbf{w}}_l\|_\infty > B_l^\circ | \mathbf{z}) \pi(\mathbf{z}) \\ &\leq \sum_{l=0}^L \mathbb{P}\left(\sum_{i=1}^{k_{l+1}} z_{li} > s_l^\circ\right) + \sum_{l=0}^L \mathbb{P}\left(\sup_{i=1, \dots, k_{l+1}} \|\bar{\mathbf{w}}_{li}\|_1 > B_l^\circ \mid \mathbf{z}\right) \end{aligned}$$

where $\tilde{\mathbf{w}}_l = (\|\bar{\mathbf{w}}_{l1}\|_1, \dots, \|\bar{\mathbf{w}}_{lk_{l+1}}\|_1)^T$ and the last inequality holds since $\Pi(\|\tilde{\mathbf{w}}_l\|_0 > s_l^\circ | \mathbf{z}) \leq 1$, $\Pi(\|\tilde{\mathbf{w}}_l\|_0 > s_l^\circ | \mathbf{z}) = 1$ iff $\sum z_{li} > s_l^\circ$ and $\pi(\mathbf{z}) \leq 1$. We will now break the proof in two parts as follows.

Part 1.

$$\sum_{l=0}^L \mathbb{P}\left(\sum_{i=1}^{k_{l+1}} z_{li} > s_l^\circ\right) = \sum_{l=0}^L \mathbb{P}\left(\sum_{i=1}^{k_{l+1}} z_{li} - k_{l+1}\lambda_l > s_l^\circ - k_{l+1}\lambda_l\right)$$

By Bernstein inequality

$$\leq \sum_{l=0}^L \exp\left(\frac{-1/2(s_l^\circ - k_{l+1}\lambda_l)^2}{k_{l+1}\lambda_l(1 - \lambda_l) + 1/3(s_l^\circ - k_{l+1}\lambda_l)}\right) \leq \sum_{l=0}^L \exp\left(\frac{-1/2(s_l^\circ - k_{l+1}\lambda_l)^2}{k_{l+1}\lambda_l + 1/3(s_l^\circ - k_{l+1}\lambda_l)}\right)$$

$$\begin{aligned}
&= \sum_{l=0}^L \exp\left(\frac{-s_l^\circ/2(1 - k_{l+1}\lambda_l/s_l^\circ)^2}{1/3(1 + 2k_{l+1}\lambda_l/s_l^\circ)}\right) \rightarrow \sum_{l=0}^L \exp\left(-\frac{3s_l^\circ}{2}\right) \quad \text{since } \frac{k_{l+1}\lambda_l}{s_l^\circ} \rightarrow 0 \text{ by (19)} \\
&= \sum_{l=0}^L \exp\left(-\frac{3n\epsilon_n^2}{4\sum u_l} + \frac{3}{2}\right) \leq 5(L+1) \exp\left(-\frac{n\epsilon_n^2}{2\sum u_l}\right) \leq \exp\left(-\frac{n\epsilon_n^2}{4\sum u_l}\right)
\end{aligned}$$

since $\sum u_l \log(5(L+1)) \sim \sum u_l \log L = o(n\epsilon_n^2)$ by (19).

Part 2.

$$\begin{aligned}
\sum_{l=0}^L \mathbb{P}\left(\sup_{i=1, \dots, k_{l+1}} \|\mathbf{w}_{li}\|_1 > B_l^\circ \mid \mathbf{z}\right) &\leq \sum_{l=0}^L \sum_{i=1}^{k_{l+1}} \mathbb{P}\left(\|\mathbf{w}_{li}\|_1 > B_l^\circ \mid \mathbf{z}\right) \\
&\leq \sum_{l=0}^L \sum_{i=1}^{k_{l+1}} \mathbb{P}\left(\|\mathbf{w}_{li}\|_\infty > \frac{B_l^\circ}{k_l + 1} \mid \mathbf{z}\right) \\
&\leq \sum_{l=0}^L \sum_{i=1}^{k_{l+1}} \sum_{j=1}^{k_{l+1}} \mathbb{P}\left(|w_{lij}| > \frac{B_l^\circ}{k_l + 1} \mid \mathbf{z}\right) \\
&\leq 2 \sum_{l=0}^L \sum_{i=1}^{k_{l+1}} \sum_{j=1}^{k_{l+1}} \exp\left(-\frac{B_l^{\circ 2}}{(k_l + 1)^2}\right) \quad \text{By concentration inequality} \\
&= 2 \sum_{l=0}^L \sum_{i=1}^{k_{l+1}} \sum_{j=1}^{k_{l+1}} \exp\left(-\exp\left(\frac{2n\epsilon_n^2}{((L+1)\sum_{j'=0}^L (s_{j'}^\circ + 1))} - 2\log(k_l + 1)\right)\right) \\
&\leq \sum_{l=0}^L \sum_{i=1}^{k_{l+1}} \sum_{j=1}^{k_{l+1}} \frac{1}{(L+1)k_{l+1}(k_l + 1)} \exp(-n\epsilon_n^2) = \exp(-n\epsilon_n^2)
\end{aligned}$$

where the third inequality holds since $|w_{lij}|$ given \mathbf{z} is bound above by a $|N(0, \sigma_0^2)|$ random variable. The above proof holds as long as

$$\exp\left(\frac{2n\epsilon_n^2}{(L+1)\sum_{j'=0}^L (s_{j'}^\circ + 1)} - 2\log(k_l + 1)\right) \geq n\epsilon_n^2 + \log(L+1) + \log k_{l+1} + \log(k_l + 1) + \log 2$$

Taking log on both sides we get

$$\left(\frac{n\epsilon_n^2}{(L+1)\sum_{j'=0}^L (s_{j'}^\circ + 1)} - \log(k_l + 1)\right) \geq \frac{1}{2} \log(n\epsilon_n^2 + \log(L+1) + \log k_{l+1} + \log(k_l + 1) + \log 2)$$

This is true since $\sum_{j'=0}^L (s_{j'}^\circ + 1) = (L+1)n\epsilon_n^2 / \sum u_l$ is bounded above by

$$\frac{n\epsilon_n^2}{(L+1)(\log(k_l + 1) + \frac{1}{2} \log(n\epsilon_n^2 + \log(L+1) + \log k_{l+1} + \log(k_l + 1) + \log 2))}$$

□

Proof of Lemma 4.3 part 1.

$$\text{Assumption : } \quad -\log \lambda_l = O\{(k_l + 1)\vartheta_l\}, \quad -\log(1 - \lambda_l) = O\{(s_l/k_{l+1})(k_l + 1)\vartheta_l\} \quad (20)$$

$$d_{\text{KL}}(P_0, P_{\boldsymbol{\theta}}) = \int_{\mathbf{x} \in [0,1]^p} \int_{y \in \mathbb{R}} \left(\log \frac{P_0(y, \mathbf{x})}{P_{\boldsymbol{\theta}}(y, \mathbf{x})} \right) P_0(y, \mathbf{x}) dy d\mathbf{x}$$

$$P_0(y, \mathbf{x}) = \frac{1}{\sqrt{2\pi\sigma_e^2}} \exp\left(-\frac{(y - \eta_0(\mathbf{x}))^2}{2\sigma_e^2}\right) \quad P_{\boldsymbol{\theta}}(y, \mathbf{x}) = \frac{1}{\sqrt{2\pi\sigma_e^2}} \exp\left(-\frac{(y - \eta_{\boldsymbol{\theta}}(\mathbf{x}))^2}{2\sigma_e^2}\right)$$

So we get,

$$\begin{aligned} d_{\text{KL}}(P_0, P_{\boldsymbol{\theta}}) &= \int_{\mathbf{x} \in [0,1]^p} \int_{y \in \mathbb{R}} \log \left(\exp \left[-\frac{(y - \eta_0(\mathbf{x}))^2}{2\sigma_e^2} + \frac{(y - \eta_{\boldsymbol{\theta}}(\mathbf{x}))^2}{2\sigma_e^2} \right] \right) P_0(y, \mathbf{x}) dy d\mathbf{x} \\ &= \int_{\mathbf{x} \in [0,1]^p} \int_{y \in \mathbb{R}} \frac{2y(\eta_0(\mathbf{x}) - \eta_{\boldsymbol{\theta}}(\mathbf{x})) - (\eta_0^2(\mathbf{x}) - \eta_{\boldsymbol{\theta}}^2(\mathbf{x}))}{2\sigma_e^2} P_0(y, \mathbf{x}) dy d\mathbf{x} \\ &= \int_{\mathbf{x} \in [0,1]^p} \frac{2\eta_0^2(\mathbf{x}) - 2\eta_0(\mathbf{x})\eta_{\boldsymbol{\theta}}(\mathbf{x}) - \eta_0^2(\mathbf{x}) + \eta_{\boldsymbol{\theta}}^2(\mathbf{x})}{2\sigma_e^2} d\mathbf{x} \\ &= \int_{\mathbf{x} \in [0,1]^p} \frac{(\eta_0(\mathbf{x}) - \eta_{\boldsymbol{\theta}}(\mathbf{x}))^2}{2} d\mathbf{x} = \frac{1}{2} \|\eta_0 - \eta_{\boldsymbol{\theta}}\|_2^2 \end{aligned} \quad (21)$$

where, $\sigma_e^2 = 1$ can be chosen w.l.o.g. Next, let $\eta_{\boldsymbol{\theta}^*}(\mathbf{x})$ be $\boldsymbol{\theta}^*$ satisfying $\arg \min_{\boldsymbol{\theta} \in \mathcal{F}(L, \mathbf{k}, \mathbf{s}, \mathbf{B})} \|\eta_{\boldsymbol{\theta}} - \eta_0\|_{\infty}^2$. Then,

$$\|\eta_{\boldsymbol{\theta}^*} - \eta_0\|_1 \leq \|\eta_{\boldsymbol{\theta}^*} - \eta_0\|_{\infty} = \sqrt{\xi} \quad (22)$$

Here, we redefine $\bar{\boldsymbol{\delta}}_l$ by considering the L_1 norms of the rows of $\bar{\mathbf{D}}_l = \bar{\mathbf{W}}_l - \bar{\mathbf{W}}_l^*$ as follows

$$\bar{\mathbf{D}}_l = (\bar{\mathbf{d}}_{l1}^{\top}, \dots, \bar{\mathbf{d}}_{lk_{l+1}}^{\top})^{\top} \quad \bar{\boldsymbol{\delta}}_l = (\|\bar{\mathbf{d}}_{l1}\|_1, \dots, \|\bar{\mathbf{d}}_{lk_{l+1}}\|_1)$$

Next we define a neighborhood $\mathcal{M}_{\sqrt{\sum r_l}}$ as follows:

$$\mathcal{M}_{\sqrt{\sum r_l}} = \left\{ \boldsymbol{\theta} : \|\bar{\mathbf{d}}_{li}\|_1 \leq \frac{\sqrt{\sum r_l} B_l}{(L+1)(\prod_{j=0}^L B_j)}, i \in \mathcal{S}_l, \|\bar{\mathbf{d}}_{li}\|_1 = 0, i \in \mathcal{S}_l^c, l = 0, \dots, L \right\}$$

where \mathcal{S}_l^c is the set where $\|\bar{\mathbf{w}}_{li}^*\|_1 = 0$, $l = 0, \dots, L$. Then, for every $\boldsymbol{\theta} \in \mathcal{M}_{\sqrt{\sum r_l}}$ using (16), we have

$$\|\eta_{\boldsymbol{\theta}} - \eta_{\boldsymbol{\theta}^*}\|_1 \leq \sqrt{\sum r_l} \quad (23)$$

Combining (22) and (23), we get for $\boldsymbol{\theta} \in \mathcal{M}_{\sqrt{\sum r_l}}$, $\|\eta_{\boldsymbol{\theta}} - \eta_0\|_1 \leq \sqrt{\sum r_l} + \sqrt{\xi}$. So we get,

$$d_{\text{KL}}(P_0, P_{\boldsymbol{\theta}}) \leq \frac{(\sqrt{\sum r_l} + \sqrt{\xi})^2}{2} \leq \sum r_l + \xi$$

Since $\boldsymbol{\theta} \in \mathcal{N}_{\sum r_l + \xi}$ for every $\boldsymbol{\theta} \in \mathcal{M}_{\sqrt{\sum r_l}}$; therefore,

$$\int_{\boldsymbol{\theta} \in \mathcal{N}_{\sum r_l + \xi}} \tilde{\pi}(\boldsymbol{\theta}) d\boldsymbol{\theta} \geq \int_{\boldsymbol{\theta} \in \mathcal{M}_{\sqrt{\sum r_l}}} \tilde{\pi}(\boldsymbol{\theta}) d\boldsymbol{\theta}$$

Let $\delta_n = (\sqrt{\sum r_l B_l}) / ((L+1)(\prod_{j=0}^L B_j))$ and $A = \{\bar{\mathbf{w}}_{li} : \|\bar{\mathbf{w}}_{li} - \bar{\mathbf{w}}_{li}^*\|_1 \leq \delta_n\}$

$$\begin{aligned}
\tilde{\Pi}(\mathcal{M}_{\sqrt{\sum r_l}}) &= \sum_{\mathbf{z}} \Pi(\mathcal{M}_{\sqrt{\sum r_l}} | \mathbf{z}) \pi(\mathbf{z}) \\
&\geq \sum_{\{\mathbf{z}: z_{li}=1, i \in \mathcal{S}_l, z_{li}=0, i \in \mathcal{S}_l^c, l=0, \dots, L\}} \Pi(\mathcal{M}_{\sqrt{\sum r_l}} | \mathbf{z}) \pi(\mathbf{z}) \\
&= \prod_{l=0}^L (1 - \lambda_l)^{k_{l+1} - s_l} \lambda_l^{s_l} \prod_{i \in \mathcal{S}_l} \mathbb{E}(\mathbb{1}_{\{\bar{\mathbf{w}}_{li} \in A\}} | z_{li} = 1) \\
&\geq \prod_{l=0}^L (1 - \lambda_l)^{k_{l+1} - s_l} \lambda_l^{s_l} \prod_{i \in \mathcal{S}_l} \int_{\bar{\mathbf{w}}_{li} \in A} \left(\frac{1}{2\pi}\right)^{\frac{k_l+1}{2}} \prod_{j=1}^{k_l+1} \exp\left(-\frac{\bar{w}_{lij}^2}{2}\right) d\bar{w}_{lij} \\
&\geq \prod_{l=0}^L (1 - \lambda_l)^{k_{l+1} - s_l} \lambda_l^{s_l} \prod_{i \in \mathcal{S}_l} \left(\frac{1}{2\pi}\right)^{\frac{k_l+1}{2}} \prod_{j=1}^{k_l+1} \int_{\bar{w}_{lij}^* - \frac{\delta_n}{k_l+1}}^{\bar{w}_{lij}^* + \frac{\delta_n}{k_l+1}} \exp\left(-\frac{\bar{w}_{lij}^2}{2}\right) d\bar{w}_{lij} \\
&= \prod_{l=0}^L (1 - \lambda_l)^{k_{l+1} - s_l} \lambda_l^{s_l} \prod_{i \in \mathcal{S}_l} \left(\frac{1}{2\pi}\right)^{\frac{k_l+1}{2}} \prod_{j=1}^{k_l+1} \frac{2\delta_n}{k_l+1} \exp\left(-\frac{\hat{w}_{lij}^2}{2}\right)
\end{aligned}$$

where the third equality follows since $\mathbb{E}(\mathbb{1}_{\{\bar{\mathbf{w}}_{li} \in A\}} | z_{li} = 0) = 1$ since $\|\bar{\mathbf{w}}_{li}^*\|_1 = 0$, for $i \in \mathcal{S}_l^c$. The last equality is by mean value theorem, $\hat{w}_{lij} \in [\bar{w}_{lij}^* - \delta_n/(k_l+1), \bar{w}_{lij}^* + \delta_n/(k_l+1)]$, thus

$$\begin{aligned}
&= \prod_{l=0}^L (1 - \lambda_l)^{k_{l+1} - s_l} \lambda_l^{s_l} \prod_{i \in \mathcal{S}_l} \exp\left(\frac{k_l+1}{2} \log \frac{1}{2\pi} + (k_l+1) \log \frac{2\delta_n}{k_l+1} - \sum_{j=1}^{k_l+1} \frac{\hat{w}_{lij}^2}{2}\right) \\
&= \exp\left[-\sum_{l=0}^L \left\{s_l \log\left(\frac{1}{\lambda_l}\right) + (k_{l+1} - s_l) \log\left(\frac{1}{1 - \lambda_l}\right) \right. \right. \\
&\quad \left. \left. + \sum_{i \in \mathcal{S}_l} \left(-\frac{k_l+1}{2} \log \frac{1}{2\pi} - (k_l+1) \log \frac{2\delta_n}{k_l+1} + \sum_{j=1}^{k_l+1} \frac{\hat{w}_{lij}^2}{2}\right)\right\}\right] \\
&= \exp\left[-\sum_{l=0}^L \left\{s_l \log\left(\frac{1}{\lambda_l}\right) + (k_{l+1} - s_l) \log\left(\frac{1}{1 - \lambda_l}\right) \right. \right. \\
&\quad \left. \left. - \frac{s_l(k_l+1)}{2} \log \frac{1}{2\pi} - s_l(k_l+1) \log \frac{2\delta_n}{k_l+1} + \sum_{i \in \mathcal{S}_l} \sum_{j=1}^{k_l+1} \frac{\hat{w}_{lij}^2}{2}\right\}\right] \tag{24}
\end{aligned}$$

Now,

$$\begin{aligned}
\sum_{l=0}^L \sum_{i \in \mathcal{S}_l} \sum_{j=1}^{k_l+1} \frac{\hat{w}_{lij}^2}{2} &\leq \frac{1}{2} \sum_{l=0}^L \sum_{i \in \mathcal{S}_l} \sum_{j=1}^{k_l+1} \max((\bar{w}_{lij}^* - \delta_n/(k_l+1))^2, (\bar{w}_{lij}^* + \delta_n/(k_l+1))^2) \\
&\leq \sum_{l=0}^L \sum_{i \in \mathcal{S}_l} \sum_{j=1}^{k_l+1} (\bar{w}_{lij}^{*2} + \delta_n^2/(k_l+1)^2) \leq \sum_{l=0}^L \sum_{i \in \mathcal{S}_l} \|\bar{\mathbf{w}}_{li}^*\|_1^2 + \sum_{l=0}^L \sum_{i \in \mathcal{S}_l} \delta_n^2/(k_l+1) \\
&\leq \sum_{l=0}^L s_l(B_l^2 + 1) \leq n \sum r_l \leq n \left(\sum r_l + \xi\right) \tag{25}
\end{aligned}$$

where the above line uses $\delta_n \rightarrow 0$. Finally

$$\begin{aligned}
& \sum_{l=0}^L \left(s_l \log \left(\frac{1}{\lambda_l} \right) + (k_{l+1} - s_l) \log \left(\frac{1}{1 - \lambda_l} \right) - \frac{s_l(k_l + 1)}{2} \log \frac{1}{2\pi} - s_l(k_l + 1) \log \frac{2\delta_n}{k_l + 1} \right) \\
& \leq \sum_{l=0}^L \left(Cnr_l + \frac{s_l(k_l + 1)}{2} \left\{ 2 \log(k_l + 1) + 2 \log(L + 1) + 2 \sum_{m=0, m \neq l}^L \log B_m - \log \sum r_l \right\} \right) \\
& \leq Cn \sum r_l \leq Cn \left(\sum r_l + \xi \right)
\end{aligned} \tag{26}$$

where the first inequality follows from (20) and expanding δ_n . The last inequality follows since $n \sum r_l \rightarrow \infty$ which implies $-\log \sum r_l = O(\log n)$. Combining (25) and (26) and replacing (24), the proof follows. \square

Proof of Lemma 4.3 part 2.

$$\text{Assumption : } \quad -\log \lambda_l = O\{(k_l + 1)\vartheta_l\}, \quad -\log(1 - \lambda_l) = O\{(s_l/k_{l+1})(k_l + 1)\vartheta_l\}$$

Suppose there exists $q \in \mathcal{Q}^{\text{MF}}$ such that

$$\begin{aligned}
d_{\text{KL}}(q, \pi) & \leq C_1 n \sum r_l, \\
\sum_{\mathbf{z}} \int_{\Theta} \|\eta_{\theta} - \eta_{\theta^*}\|_2^2 q(\theta, \mathbf{z}) d\theta & \leq \sum r_l.
\end{aligned} \tag{27}$$

Recall $\theta^* = \arg \min_{\theta \in \Theta(L, p, s, B)} \|\eta_{\theta} - \eta_0\|_{\infty}^2$. By relation (21),

$$\begin{aligned}
\sum_{\mathbf{z}} \int n d_{\text{KL}}(P_0, P_{\theta}) q(\theta, \mathbf{z}) d\theta & = \sum_{\mathbf{z}} \frac{n}{2} \int \|\eta_0 - \eta_{\theta}\|_2^2 q(\theta, \mathbf{z}) d\theta \\
& \leq \frac{n}{2} \sum_{\mathbf{z}} \int \|\eta_{\theta^*} - \eta_{\theta}\|_2^2 q(\theta, \mathbf{z}) d\theta + \frac{n}{2} \|\eta_{\theta^*} - \eta_0\|_{\infty}^2 \\
& \leq Cn \left(\sum r_l + \xi \right)
\end{aligned}$$

where the above relation is due to (27) which will complete the proof.

We next construct $q \in \mathcal{Q}^{\text{MF}}$ as

$$\bar{w}_{lij} | z_{li} \sim z_{li} \mathcal{N}(\bar{w}_{lij}^*, \sigma_l^2) + (1 - z_{li}) \delta_0, \quad z_{li} \sim \text{Bern}(\gamma_{li}^*) \quad \gamma_{li}^* = \mathbb{1}(\|\mathbf{w}_{li}^*\|_1 \neq 0)$$

where $\sigma_l^2 = \frac{s_l}{8n(L+1)} (4^{L-l} (k_l + 1) \log(k_{l+1} 2^{k_l+1}) \prod_{m=0, m \neq l}^L B_m^2)^{-1}$.

We next consider the relation (18) in Lemma A.7.

We upper bound the expectation of the supremum of L_1 norm of multivariate Gaussian variables:

$$\int \widetilde{W}_l q(\theta, \mathbf{z}) d\theta \leq \int \sup_i \|\bar{\mathbf{w}}_{li} - \bar{\mathbf{w}}_{li}^*\|_1 q(\theta | \mathbf{z}) d\theta \leq \int \sup_i \|\bar{\mathbf{w}}_{li} - \bar{\mathbf{w}}_{li}^*\|_1 q(\theta | \mathbf{z} = \mathbf{1}) d\theta$$

since $q(\mathbf{z}) \leq 1$. If $z_{li} = 1$, then $\|\bar{\mathbf{w}}_{li} - \bar{\mathbf{w}}_{li}^*\|_1 = 0$, thus the above integral is maximized at $\mathbf{z} = \mathbf{1}$ where $\mathbf{z} = \mathbf{1}$ indicates all neurons are present in the network. In this case, all w_{li} are nothing but independent Gaussian random variables. In this direction we make use of concentration inequalities similar to the proof of theorem

2 in Chérief-Abdellatif (2020). Let, $Y = \sup_i \|\bar{\mathbf{w}}_{li} - \bar{\mathbf{w}}_{li}^*\|_1$.

$$\begin{aligned} \exp(t\mathbb{E}Y) &\leq \mathbb{E}(\exp(tY)) = \mathbb{E}[\sup_i \exp(t\|\bar{\mathbf{w}}_{li} - \bar{\mathbf{w}}_{li}^*\|_1)] \\ &\leq \sum_{i=1}^{k_{l+1}} \mathbb{E}[\exp(t \sum_{j=1}^{k_{l+1}} |\bar{w}_{lij} - \bar{w}_{lij}^*|)] = \sum_{i=1}^{k_{l+1}} \prod_{j=1}^{k_{l+1}} \mathbb{E}[\exp(t|\bar{w}_{lij} - \bar{w}_{lij}^*|)] \\ &= \sum_{i=1}^{k_{l+1}} \prod_{j=1}^{k_{l+1}} 2 \exp\left[\frac{\sigma_l^2 t^2}{2}\right] \Phi(\sigma_l t) \leq k_{l+1} 2^{k_{l+1}} \exp\left[(k_l + 1) \frac{\sigma_l^2 t^2}{2}\right] \end{aligned}$$

Thus, $\mathbb{E}Y \leq (\log(k_{l+1} 2^{k_{l+1}}) + (k_l + 1)\sigma_l^2 t^2/2)/t$. Let $t = (1/\sigma_l)\sqrt{(2/(k_l + 1)) \log(k_{l+1} 2^{k_{l+1}})}$,

$$\begin{aligned} \mathbb{E}Y &\leq \sigma_l \sqrt{\frac{k_l + 1}{2}} \left[\sqrt{\log(k_{l+1} 2^{k_{l+1}})} + \sqrt{\log(k_{l+1} 2^{k_{l+1}})} \right] \\ &= \sqrt{2\sigma_l^2 (k_l + 1) \log(k_{l+1} 2^{k_{l+1}})} \leq \sqrt{4\sigma_l^2 (k_l + 1) \log(k_{l+1} 2^{k_{l+1}})} \end{aligned}$$

Similarly,

$$\int \widetilde{W}_l^2 q(\boldsymbol{\theta}, \mathbf{z}) d\boldsymbol{\theta} = \int \sup_i (\|\bar{\mathbf{w}}_{li} - \bar{\mathbf{w}}_{li}^*\|_1)^2 q(\boldsymbol{\theta}, \mathbf{z}) d\boldsymbol{\theta} \leq \int \sup_i (\|\bar{\mathbf{w}}_{li} - \bar{\mathbf{w}}_{li}^*\|_1)^2 q(\boldsymbol{\theta} | \mathbf{z} = \mathbf{1})$$

Let, $Y' = \sup_i (\|\bar{\mathbf{w}}_{li} - \bar{\mathbf{w}}_{li}^*\|_1)^2$.

$$\begin{aligned} \exp(t\mathbb{E}Y') &\leq \mathbb{E}(\exp(tY')) = \mathbb{E}[\sup_i \exp(t\|\bar{\mathbf{w}}_{li} - \bar{\mathbf{w}}_{li}^*\|_1^2)] \\ &\leq \sum_{i=1}^{k_{l+1}} \mathbb{E}[\exp(t(\sum_{j=1}^{k_{l+1}} |\bar{w}_{lij} - \bar{w}_{lij}^*|)^2)] \leq \sum_{i=1}^{k_{l+1}} \mathbb{E}[\exp(t(k_l + 1) \sum_{j=1}^{k_{l+1}} (\bar{w}_{lij} - \bar{w}_{lij}^*)^2)] \\ &= \sum_{i=1}^{k_{l+1}} \prod_{j=1}^{k_{l+1}} \mathbb{E}[\exp(t(k_l + 1)(\bar{w}_{lij} - \bar{w}_{lij}^*)^2)] = \sum_{i=1}^{k_{l+1}} \prod_{j=1}^{k_{l+1}} \left(\frac{1}{1 - 2t(k_l + 1)\sigma_l^2} \right)^{\frac{1}{2}} \\ &\leq k_{l+1} \left(\frac{1}{1 - 2t(k_l + 1)\sigma_l^2} \right)^{\frac{k_{l+1}}{2}} \end{aligned}$$

Thus, $\mathbb{E}Y' \leq (\log k_{l+1} - ((k_l + 1)/2) \log(1 - 2t(k_l + 1)\sigma_l^2))/t$. Let $t = 1/(4\sigma_l^2 (k_l + 1))$,

$$\begin{aligned} \mathbb{E}Y' &\leq 4\sigma_l^2 (k_l + 1) \left[\log k_{l+1} + \left(\frac{k_l + 1}{2} \right) \log 2 \right] = 4\sigma_l^2 (k_l + 1) \log(k_{l+1} 2^{\frac{k_l + 1}{2}}) \\ &\leq 4\sigma_l^2 (k_l + 1) \log(k_{l+1} 2^{k_{l+1}}) \end{aligned}$$

Next we also get,

$$\int (\widetilde{W}_l + B_l) q(\boldsymbol{\theta}, \mathbf{z}) d\boldsymbol{\theta} = \int \widetilde{W}_l q(\boldsymbol{\theta}, \mathbf{z}) d\boldsymbol{\theta} + B_l \leq \sqrt{4\sigma_l^2 (k_l + 1) \log(k_{l+1} 2^{k_{l+1}})} + B_l \leq 2B_l$$

$$\begin{aligned} \int (\widetilde{W}_l + B_l)^2 q(\boldsymbol{\theta}, \mathbf{z}) d\boldsymbol{\theta} &= \int \widetilde{W}_l^2 q(\boldsymbol{\theta}, \mathbf{z}) d\boldsymbol{\theta} + 2B_l \int \widetilde{W}_l q(\boldsymbol{\theta}, \mathbf{z}) d\boldsymbol{\theta} + B_l^2 \\ &\leq 4\sigma_l^2 (k_l + 1) \log(k_{l+1} 2^{k_{l+1}}) + 2B_l \sqrt{4\sigma_l^2 (k_l + 1) \log(k_{l+1} 2^{k_{l+1}})} + B_l^2 \leq 4B_l^2 \end{aligned}$$

$$\begin{aligned}
& \int \widetilde{W}_l(\widetilde{W}_l + B_l)q(\boldsymbol{\theta}, \mathbf{z})d\boldsymbol{\theta} = \int \widetilde{W}_l^2 q(\boldsymbol{\theta}, \mathbf{z})d\boldsymbol{\theta} + B_l \int \widetilde{W}_l q(\boldsymbol{\theta}, \mathbf{z})d\boldsymbol{\theta} \\
& \leq 4\sigma_l^2(k_l + 1) \log(k_{l+1}2^{k_l+1}) + B_l \sqrt{4\sigma_l^2(k_l + 1) \log(k_{l+1}2^{k_l+1})} \\
& \leq \sqrt{4\sigma_l^2(k_l + 1) \log(k_{l+1}2^{k_l+1})} \left(\sqrt{4\sigma_l^2(k_l + 1) \log(k_{l+1}2^{k_l+1})} + B_l \right) \\
& \leq 2B_l \sqrt{4\sigma_l^2(k_l + 1) \log(k_{l+1}2^{k_l+1})}
\end{aligned}$$

since $\sqrt{4\sigma_l^2(k_l + 1) \log(k_{l+1}2^{k_l+1})}$ is bounded above by

$$\begin{aligned}
& \sqrt{\frac{4s_l}{8n(L+1)} \left(4^{L-l}(k_l + 1) \log(k_{l+1}2^{k_l+1}) \prod_{m=0, m \neq l}^L B_m^2 \right)^{-1}} (k_l + 1) \log(k_{l+1}2^{k_l+1}) \\
& = B_l \sqrt{\frac{s_l}{2n(L+1)} \left(4^{L-l} \prod_{m=0}^L B_m^2 \right)^{-1}} \leq B_l, \text{ The quantity in square root } < 1 \text{ for large } n.
\end{aligned}$$

Let $b_j = (k_j + 1) \log(k_{j+1}2^{k_j+1})$. From relation (18), we get

$$\begin{aligned}
& \int \|\eta_{\boldsymbol{\theta}} - \eta_{\boldsymbol{\theta}^*}\|_2^2 q(\boldsymbol{\theta}, \mathbf{z})d\boldsymbol{\theta} \leq \sum_{j=0}^L c_{j-1}^2 (4\sigma_j^2 b_j) \left(\prod_{m=j+1}^L 4B_m^2 \right) \\
& + 2 \sum_{j=0}^L \sum_{j'=0}^{j-1} c_{j-1} c_{j'-1} 2B_j \sqrt{4\sigma_j^2 b_j} \left(\prod_{m=j+1}^L 4B_m^2 \right) \sqrt{4\sigma_{j'}^2 b_{j'}} \left(\prod_{m=j'+1}^{j-1} 2B_m \right) \\
& = 4 \sum_{j=0}^L 4^{L-j} \sigma_j^2 b_j \left(\prod_{m=0}^{j-1} B_m^2 \right) \left(\prod_{m=j+1}^L B_m^2 \right) \\
& + 8 \sum_{j=0}^L \sum_{j'=0}^{j-1} \left(\prod_{m=0}^{j-1} B_m \right) \left(\prod_{m=0}^{j-1} B_m \right) 2B_j \left(\prod_{m=j+1}^L 4B_m^2 \right) \left(\prod_{m=j'+1}^{j-1} 2B_m \right) \sqrt{\sigma_j^2 b_j} \sqrt{\sigma_{j'}^2 b_{j'}} \\
& = 4 \sum_{j=0}^L 2^{2L-2j} \sigma_j^2 b_j \prod_{m=0, m \neq j}^L B_m^2 \\
& + 8 \sum_{j=0}^L \sum_{j'=0}^{j-1} 4^{L-j} 2^{j-j'} \left(\prod_{m=0}^{j-1} B_m \right) \left(\prod_{m=0}^{j-1} B_m \right) \left(\prod_{m=j+1}^L B_m \right) \left(\prod_{m=j'+1}^L B_m \right) \sqrt{\sigma_j^2 b_j} \sqrt{\sigma_{j'}^2 b_{j'}} \\
& = 4 \sum_{j=0}^L 2^{2L-2j} \sigma_j^2 b_j \left(\prod_{m=0, m \neq j}^L B_m^2 \right) \\
& + 8 \sum_{j=0}^L \sum_{j'=0}^{j-1} 2^{L-j} 2^{L-j'} \left(\prod_{m=0, m \neq j}^L B_m \right) \left(\prod_{m=0, m \neq j'}^L B_m \right) \sqrt{\sigma_j^2 b_j} \sqrt{\sigma_{j'}^2 b_{j'}} \\
& = 4 \left(\sum_{j=0}^L 2^{L-j} \sqrt{\sigma_j^2 b_j} \left(\prod_{m=0, m \neq j}^L B_m \right) \right)^2 = 4 \left(\sum_{j=0}^L \sqrt{\frac{s_j}{8n(L+1)}} \right)^2 \\
& = \frac{1}{2n(L+1)} \left(\sum_{j=0}^L \sqrt{s_j} \right)^2 \leq \frac{\sum_{j=0}^L s_j}{2n} \leq \sum_{j=0}^L r_l
\end{aligned}$$

This concludes the proof of (27). Next,

$$\begin{aligned}
d_{\text{KL}}(q, \pi) &\leq \log \frac{1}{\pi(\mathbf{z})} + \mathbb{1}(\mathbf{z} = \gamma^*) d_{\text{KL}} \left(\left\{ \prod_{l=0}^{L-1} \prod_{i=1}^{k_{l+1}} \prod_{j=1}^{k_{l+1}} \left\{ \gamma_{li}^* \mathcal{N}(\bar{w}_{lij}^*, \sigma_l^2) + (1 - \gamma_{li}^*) \delta_0 \right\} \right. \right. \\
&\quad \left. \left. \prod_{j=1}^{k_L+1} \mathcal{N}(\bar{w}_{Lj}^*, \sigma_L^2) \right\}, \left\{ \prod_{l=0}^{L-1} \prod_{i=1}^{k_{l+1}} \prod_{j=1}^{k_{l+1}} \left\{ z_{li} \mathcal{N}(0, \sigma_0^2) + (1 - z_{li}) \delta_0 \right\} \prod_{j=1}^{k_L+1} \mathcal{N}(0, \sigma_0^2) \right\} \right) \\
&= \log \frac{1}{\prod_{l=0}^{L-1} \lambda_l^{s_l} (1 - \lambda_l)^{k_{l+1} - s_l}} + \sum_{l=0}^{L-1} \sum_{i=1}^{k_{l+1}} \sum_{j=1}^{k_{l+1}} d_{\text{KL}} \left(\gamma_{li}^* \mathcal{N}(\bar{w}_{lij}^*, \sigma_l^2) + (1 - \gamma_{li}^*) \delta_0, \right. \\
&\quad \left. \gamma_{li}^* \mathcal{N}(0, \sigma_0^2) + (1 - \gamma_{li}^*) \delta_0 \right) + \sum_{j=1}^{k_L+1} d_{\text{KL}} \left(\mathcal{N}(\bar{w}_{Lj}^*, \sigma_L^2), \mathcal{N}(0, \sigma_0^2) \right) \\
&= \sum_{l=0}^{L-1} \left(s_l \log \frac{1}{\lambda_l} + (k_{l+1} - s_l) \log \frac{1}{1 - \lambda_l} \right) + \sum_{l=0}^{L-1} \sum_{i=1}^{k_{l+1}} \sum_{j=1}^{k_{l+1}} \gamma_{li}^* \left\{ \frac{1}{2} \log \frac{\sigma_0^2}{\sigma_l^2} + \frac{\sigma_l^2 + \bar{w}_{lij}^{*2}}{2\sigma_0^2} - \frac{1}{2} \right\} \\
&\quad + \sum_{j=1}^{k_L+1} \left\{ \frac{1}{2} \log \frac{\sigma_0^2}{\sigma_L^2} + \frac{\sigma_L^2 + \bar{w}_{Lj}^{*2}}{2\sigma_0^2} - \frac{1}{2} \right\} \\
&\leq \sum_{l=0}^{L-1} Cnr_l + \sum_{l=0}^{L-1} \frac{s_l k_l + s_l}{2} \left[\frac{\sigma_l^2}{\sigma_0^2} + \frac{B_l^2}{\sigma_0^2 (k_l + 1)} - 1 + \log \frac{\sigma_0^2}{\sigma_l^2} \right] + \frac{k_L + 1}{2} \left[\frac{\sigma_L^2}{\sigma_0^2} + \frac{B_L^2}{\sigma_0^2 (k_L + 1)} - 1 + \log \frac{\sigma_0^2}{\sigma_L^2} \right]
\end{aligned}$$

where the first inequality follows from Lemma A.4. The inequality in the above line uses $\sum_{j=1}^{k_{l+1}} \bar{w}_{lij}^{*2} \leq B_l^2$ and similar to the proof of Lemma 4.1 in Bai et al. (2020) uses (20).

Let $\sigma_0^2 = 1$ and it could be easily derived that $\sigma_l^2 \leq 1$.

$$\begin{aligned}
d_{\text{KL}}(q, \pi) &\leq \sum_{l=0}^{L-1} Cnr_l + \sum_{l=0}^{L-1} \frac{s_l}{2} (k_l + 1) \left[\frac{B_l^2}{k_l + 1} - \log \sigma_l^2 \right] + \frac{(k_L + 1)}{2} \left[\frac{B_L^2}{k_L + 1} - \log \sigma_L^2 \right] \\
&= \sum_{l=0}^{L-1} Cnr_l + \sum_{l=0}^{L-1} \frac{s_l}{2} (k_l + 1) \left[\frac{B_l^2}{k_l + 1} - \log \left(\frac{s_l}{8n(L+1)} \left[4^{L-l} b_l \prod_{m=0, m \neq l}^L B_m^2 \right]^{-1} \right) \right] \\
&\quad + \frac{(k_L + 1)}{2} \left[\frac{B_L^2}{k_L + 1} - \log \left(\frac{1}{8n(L+1)} \left[b_L \prod_{m=0, m \neq L}^L B_m^2 \right]^{-1} \right) \right] \\
&= \sum_{l=0}^{L-1} Cnr_l + \sum_{l=0}^{L-1} \frac{s_l}{2} (k_l + 1) \left[\frac{B_l^2}{k_l + 1} - \log \left(\frac{s_l}{8n(L+1)} \left[4^{L-l} b_l \prod_{m=0, m \neq l}^L B_m^2 \right]^{-1} \right) \right] \\
&= \sum_{l=0}^{L-1} Cnr_l + \sum_{l=0}^{L-1} \frac{s_l}{2} B_l^2 + \sum_{l=0}^{L-1} \frac{s_l}{2} (k_l + 1) \log \left(\frac{8n(L+1)}{s_l} \right) \\
&\quad + \sum_{l=0}^L s_l (k_l + 1) (L - l) \log 2 + \sum_{l=0}^L \frac{s_l}{2} (k_l + 1) \log (k_l + 1) \\
&\quad + \sum_{l=0}^L \frac{s_l}{2} (k_l + 1) \log \left(\log(k_{l+1} 2^{k_{l+1}}) \right) + \sum_{l=0}^L s_l (k_l + 1) \left(\sum_{m=0, m \neq l}^L \log B_m \right)
\end{aligned}$$

$$\begin{aligned}
&\leq \sum_{l=0}^{L-1} Cnr_l + \sum_{l=0}^L \frac{s_l}{2} B_l^2 + \sum_{l=0}^L \frac{s_l}{2} (k_l + 1) \log \left(\frac{8n(L+1)}{s_l} \right) + L \sum_{l=0}^L s_l (k_l + 1) \\
&\quad + \sum_{l=0}^L \frac{s_l}{2} (k_l + 1) (\log(k_l + 1) + \log(k_{l+1} + k_l + 1)) + \sum_{l=0}^L s_l (k_l + 1) \left(\sum_{m=0, m \neq l}^L \log B_m \right) \\
&\leq \sum_{l=0}^{L-1} Cnr_l + \sum_{l=0}^L \frac{s_l}{2} B_l^2 + \sum_{l=0}^L \frac{s_l}{2} (k_l + 1) \log \left(\frac{8n(L+1)}{s_l} \right) + L \sum_{l=0}^L s_l (k_l + 1) \\
&\quad + \sum_{l=0}^L s_l (k_l + 1) \log(k_{l+1} + k_l + 1) + \sum_{l=0}^L s_l (k_l + 1) \left(\sum_{m=0, m \neq l}^L \log B_m \right) \\
&\leq \sum_{l=0}^{L-1} Cnr_l + \sum_{l=0}^L s_l (k_l + 1) \left[\frac{B_l^2}{2(k_l + 1)} + \left(\sum_{m=0, m \neq l}^L \log B_m \right) + L + \log(k_{l+1} + k_l + 1) \right. \\
&\quad \left. + \frac{1}{2} \log \left(\frac{8n(L+1)}{s_l} \right) \right] \\
&\leq \sum_{l=0}^{L-1} (C + C')nr_l + C'nr_L \\
&\quad + \sum_{l=0}^L s_l (k_l + 1) \left[\frac{B_l^2}{k_l + 1} + \left(\sum_{m=0, m \neq l}^L \log B_m \right) + L + \log(k_{l+1} + k_l + 1) + \log \left(\frac{n}{s_l} \right) \right] \\
&\leq \sum_{l=0}^{L-1} (C + C')nr_l + C'nr_L + \sum_{l=0}^L s_l (k_l + 1) \vartheta_l \leq C_1 n \sum_{l=0}^L r_l
\end{aligned}$$

This concludes the proof of (27). \square

Proof of Corollary 4.5

The proof is a direct consequence of Theorem 4.4 in the main paper as long as assumptions of Lemma 4.2 and Lemma 4.3 parts 1 and 2 hold when $\sigma_0^2 = 1$, $-\log \lambda_l = \log(k_{l+1}) + C_l(k_l + 1)\vartheta_l$ and $\epsilon_n = \sqrt{(\sum_{l=0}^L r_l + \xi) \sum_{l=0}^L u_l}$. This what we show next.

Verifying assumption (19) under Proof of Lemma 4.2: Note, $\sum u_l = O(\epsilon_n^2)$, thus

$$\sum u_l \log L = o(n\epsilon_n^2) \iff \log L = o(n(\sum r_l + \xi))$$

which is indeed true since $\log L = o(L^2)$ and $L^2 \leq n \sum r_l$. We will show that $(k_{l+1}\lambda_l)/s_l^\circ \rightarrow 0$. With $\lambda_l = (1/k_{l+1}) \exp(-C_l(k_l + 1)\vartheta_l)$,

$$\begin{aligned}
\frac{k_{l+1}\lambda_l}{s_l^\circ} &\leq \frac{\sum u_l \exp(-C(k_l + 1)\vartheta_l)}{n\epsilon_n^2} = \frac{\exp(-C(k_l + 1)\vartheta_l + \log \sum u_l)}{n\epsilon_n^2} \\
&\leq \frac{\exp(-C(k_l + 1)\vartheta_l + \vartheta_l)}{n\epsilon_n^2} \rightarrow 0
\end{aligned}$$

where the above relation holds since $\log \sum u_l \leq \vartheta_l$, $\vartheta_l \rightarrow \infty$, $k_l \rightarrow \infty$ and $n\epsilon_n^2 \rightarrow \infty$.

Verifying assumption (20) under Proof of Lemma 4.3 part 1. and part 2. Note,

$$-\log \lambda_l = \log(k_{l+1}) + C_l(k_l + 1)\vartheta_l \leq \vartheta_l + C_l(k_l + 1)\vartheta_l = O\{(k_l + 1)\vartheta_l\}$$

And then,

$$1 - \lambda_l = 1 - \exp(-C_l \vartheta_l (k_l + 1)) / k_{l+1}$$

$$-\log(1 - \lambda_l) \sim \exp(-C_l \vartheta_l (k_l + 1)) / k_{l+1} = O\{(k_l + 1) s_l \vartheta_l / k_{l+1}\}$$

since $\exp(-C_l \vartheta_l (k_l + 1)) \rightarrow 0$ and $(k_l + 1) s_l \vartheta_l \rightarrow \infty$. □

B Additional numerical experiments details

B.1 Variational parameters initialization

We initialize the γ_{lj} 's at a value close to 1 for all of our experiments. This ensures that at epoch 0, we have a fully connected deep neural network. This also warrants that most of the weights do not get pruned off at a very early stage of training which might lead to bad performance. The variational parameters $\mu_{ljj'}$ are initialized using $U(-0.6, 0.6)$ for simulation and UCI regression examples whereas for classification Kaiming uniform initialization (He et al., 2015) is used. Moreover, $\sigma_{ljj'}$ are reparameterized using softplus function: $\sigma_{ljj'} = \log(1 + \exp(\rho_{ljj'}))$ and $\rho_{ljj'}$ are initialized using a constant value of -6. This keeps initial values of $\sigma_{ljj'}$ close to 0 ensuring that the initial values of network weights stay close to Kaiming uniform initialization.

B.2 Hyperparameters for training

We keep MC sample size (S) to be 1 during training. We choose learning rate of 3×10^{-3} , batch size of 400, and 10000 epochs in the 20 neurons case of simulation study-I. We use learning rate of 10^{-3} , batch size of 400, and 20000 epochs in the 100 neurons case of simulation study-II. Next, we use learning rate of 5×10^{-3} , full batch, and 10000 epochs for simulation study-II. In UCI regression datasets, we choose batch size = 128 and run 500 epochs for *Concrete*, *Wine*, *Power Plant*, 800 epochs for *Kin8nm*. For *Protein* and *Year* datasets, we choose batch size of 256 and run 100 epochs. For all the UCI regression datasets we keep learning rate of 10^{-3} . The Adam algorithm is chosen for optimization of model parameters.

B.3 Fine tuning of constant in prior inclusion probability expression

Recall the layer-wise prior inclusion probabilities: $\lambda_l = (1/k_{l+1}) \exp(-C_l (k_l + 1) \vartheta_l)$ from the Corollary 4.5. In our numerical experiments, we use this expression to choose an optimal value of λ_l in each layer of a given network. The λ_l varies as we vary our constant C_l and we next describe how is C_l chosen. The influence of C_l is mainly due to the $k_l + 1$ term and $B_l^2 / (k_l + 1)$ from ϑ_l term. We ensure that each incoming weight and bias onto the node from layer $l + 1$ is bounded by 1 which leads us to choose B_l to be $k_l + 1$. So the leading term from $(k_l + 1) \vartheta_l$ is $(k_l + 1)$ and C_l has to be chosen such that we avoid making exponential term from λ_l expression close to 0. In our experiments we choose C_l values in the negative order of 10 such that prior inclusion probabilities do not fall below 10^{-50} . If we instead choose a λ_l value very close to 0 then we might prune off all the nodes in each layer or might make the training unstable which is not ideal. Overall the aforementioned strategy of choosing C_l constant values ensure reasonable values for the λ_l in each layer.

B.4 Simulation study I: extra details

First we provide the network parameters used to generate the data for this simulation experiment. The edge weights in the underlying 2-2-1 network are as follows: $\mathbf{W}_0 = \{w_{011} = 10, w_{012} = 15, w_{021} = -15, w_{022} = 10\}$; $\mathbf{W}_1 = \{w_{111} = -3, w_{121} = 3\}$ and $\mathbf{v}_0 = \{v_{01} = -5, v_{02} = 5\}$; $\mathbf{v}_1 = \{v_{11} = 4\}$.

Next we provide additional results demonstrating the model selection ability of our SS-IG approach in a wider network consisting of 100 nodes in the single hidden layer structure considered in the main paper.

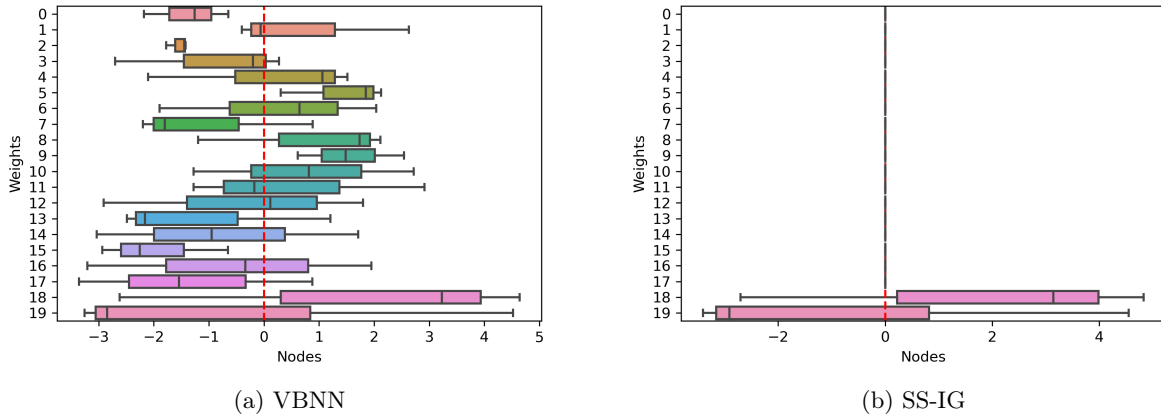


Figure 4: Node-wise weight magnitudes recovered by VBNN and proposed SS-IG model in the synthetic regression data generated using 2-2-1 network. The boxplots show the distribution of incoming weights into a given hidden layer node. Only the 20 nodes with the largest edge weights are displayed.

B.5 Fashion-MNIST (CNN extension)

Next, we evaluate the empirical performance of our model in another sophisticated image classification task presented through Fashion-MNIST dataset. Specifically we extend our model to convolutional neural network (CNN) by replacing its fully connected block by our model. We preprocessed images in the dataset using random horizontal flip. We consider 2-Conv-2-FC neural network: convolutional layer feature maps are set at 32 and 64 with filter sizes 5×5 and 3×3 . We keep padding of size 2 for each layer and 2×2 max pooling layer is applied on each feature map. The flattened feature layer with size 4096 serves as input to the fully connected block, where each layer has 4096 neurons. We use swish activation for each layer in our model instead of commonly used ReLU to avoid dying neuron problem discussed in the main paper. We keep batch size of 1024 and learning rate of 5×10^{-4} for our SS-IG model. We compare our model against dense VBNN model with ReLU activations which does not sparsify and serves as a baseline. For VBNN we use batch size of 256 and learning rate of 5×10^{-4} which we found to yield the best performance. We train both the models over 3000 epochs using Adam optimizer.

Figure 5, illustrates the results. We observe that our model learns sparse structure at a fast rate and reaches stable sparsity levels in each layer after 400 epochs (figure 5b). Our model prunes away more than 99.7% nodes from the first layer and more than 98% nodes from the second layer. However, learning sparse network affects the predictive accuracy as shown in figure 5a. As our model is pruning away extra capacity of the dense network, the predictive performance decreases at first but it slowly improves and reaches a steady level close to densely connected network of VBNN. These results demonstrate the significant network compression achieved by our model without compromising the predictive performance. Therefore, our method in practical setting could help achieve low latency and reduced storage during end-user deployment phase.

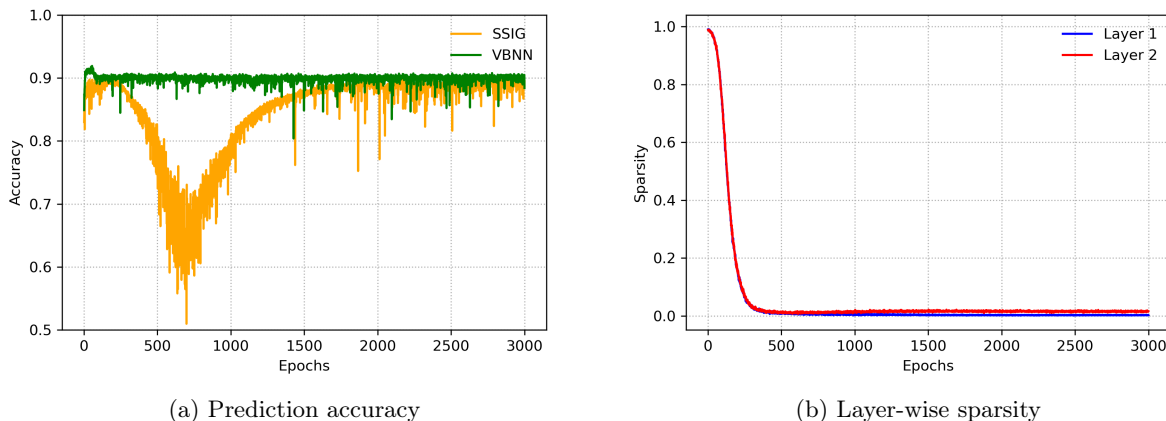


Figure 5: Fashion-MNIST experiment results.

References

- Alvarez, J. M. and Salzman, M. (2016), “Learning the Number of Neurons in Deep Networks,” in Proceedings of the 30th Advances in Neural Information Processing Systems (NIPS 2016), Barcelona, Spain.
- Bai, J., Song, Q., and Cheng, G. (2020), “Efficient Variational Inference for Sparse Deep Learning with Theoretical Guarantee,” in Proceedings of the 34th Advances in Neural Information Processing Systems (NeurIPS 2020), pp. 466–476, Vancouver, Canada.
- Bhattacharya, S. and Maiti, T. (2021), “Statistical foundation of Variational Bayes neural networks,” Neural Networks, 137, 151–173.
- Blei, D. M. and Lafferty, J. D. (2007), “A correlated topic model of Science,” The Annals of Applied Statistics, 1, 17–35.
- Blei, D. M., Kucukelbir, A., and McAuliffe, J. D. (2017), “Variational Inference: A Review for Statisticians,” Journal of the American Statistical Association, 112, 859–877.
- Blundell, C., Cornebise, J., Kavukcuoglu, K., and Wierstra, D. (2015), “Weight Uncertainty in Neural Network,” in Proceedings of Machine Learning Research, vol. 37, pp. 1613–1622, PMLR.
- Cannings, T. I. and Samworth, R. J. (2017), “Random-projection ensemble classification,” Journal of the Royal Statistical Society: Series B (Statistical Methodology), 79, 959–1035.
- Chérif-Abdellatif, B.-E. (2020), “Convergence Rates of Variational Inference in Sparse Deep Learning,” in Proceedings of the 37th International Conference on Machine Learning (ICML-2020), vol. 119, pp. 1831–1842, Vienna, Austria.
- Chérif-Abdellatif, B.-E. and Alquier, P. (2018), “Consistency of variational Bayes inference for estimation and model selection in mixtures,” Electronic Journal of Statistics, 12, 2995 – 3035.
- Dua, D. and Graff, C. (2017), “UCI Machine Learning Repository,” <http://archive.ics.uci.edu/ml>.

- Elfwing, S., Uchibe, E., and Doya, K. (2018), “Sigmoid-weighted linear units for neural network function approximation in reinforcement learning,” Neural Networks, 107, 3–11, Special issue on deep reinforcement learning.
- Frankle, J. and Carbin, M. (2019), “The Lottery Ticket Hypothesis: Finding Sparse, Trainable Neural Networks,” in International Conference on Learning Representations (ICLR 2019), New Orleans, USA.
- Friedman, J., Hastie, T., and Tibshirani, R. (2009), The elements of statistical learning, Springer series in statistics., Springer, New York.
- Ghosal, S. and van der Vaart, A. W. (2007), “Convergence rates of posterior distributions for noniid observations,” The Annals of Statistics, 35, 192 – 223.
- Ghosh, S., Yao, J., and Doshi-Velez, F. (2019), “Model Selection in Bayesian Neural Networks via Horseshoe Priors,” Journal of Machine Learning Research, pp. 1–46.
- Grenander, U. (1981), Abstract Inference, Wiley, New York.
- Han, S., Mao, H., and Dally, W. J. (2016), “Deep Compression: Compressing Deep Neural Network with Pruning, Trained Quantization and Huffman Coding,” in 4th International Conference on Learning Representations (ICLR-2016), San Juan, Puerto Rico.
- He, K., Zhang, X., Ren, S., and Sun, J. (2015), “Delving Deep into Rectifiers: Surpassing Human-Level Performance on ImageNet Classification,” in IEEE International Conference on Computer Vision (ICCV-2015), pp. 1026–1034.
- Hernandez-Lobato, J. M. and Adams, R. (2015), “Probabilistic Backpropagation for Scalable Learning of Bayesian Neural Networks,” in Proceedings of the 32nd International Conference on Machine Learning (ICML-2015), pp. 1861–1869, Lille, France.
- Hinton, G. E. and Van Camp, D. (1993), “Keeping the neural networks simple by minimizing the description length of the weights,” in Proceedings of the sixth annual conference on Computational Learning Theory (COLT-1993), p. 5–13, Santa Cruz, USA.
- Jang, E., Gu, S., and Poole, B. (2017), “Categorical Reparameterization with Gumbel-Softmax,” in 5th International Conference on Learning Representations (ICLR 2017), Toulon, France.
- Jordan, M. I., Ghahramani, Z., Jaakkola, T. S., and Sau, L. K. (1999), “An Introduction to Variational Methods for Graphical Models,” Machine Learning, 37, 183–233.
- Kingma, D. P. and Ba, J. (2015), “Adam: A Method for Stochastic Optimization,” in 3rd International Conference on Learning Representations, ICLR 2015, San Diego, USA.
- Lee, H. K. H. (2000), “Consistency of posterior distributions for neural networks,” Neural Networks, 13, 629–642.
- Louizos, C., Ullrich, K., and Welling, M. (2017), “Bayesian Compression for Deep Learning,” in Proceedings of the 30th Advances in Neural Information Processing Systems (NIPS 2017), pp. 3288–3298, Long Beach, CA, USA.
- Lu, L., Shin, Y., Su, Y., and Em Karniadakis, G. (2020), “Dying ReLU and Initialization: Theory and Numerical Examples,” Communications in Computational Physics, 28, 1671–1706.

- Maddison, C. J., Mnih, A., and Teh, Y. W. (2017), “The Concrete Distribution: A Continuous Relaxation of Discrete Random Variables,” in 5th International Conference on Learning Representations (ICLR 2017), Toulon, France.
- Mitchell, T. J. and Beauchamp, J. J. (1988), “Bayesian Variable Selection in Linear Regression,” Journal of the American Statistical Association, 83, 1023–1032.
- Molchanov, D., Ashukha, A., and Vetrov, D. (2017), “Variational Dropout Sparsifies Deep Neural Networks,” in Proceedings of the 34th International Conference on Machine Learning (ICML-2017), vol. 70, p. 2498–2507, Sydney, NSW, Australia.
- Mozer, M. C. and Smolensky, P. (1988), “Skeletonization: A technique for trimming the fat from a network via relevance assessment,” in Advances in Neural Information Processing Systems 1, pp. 107–115, Denver, USA.
- Neklyudov, K., Molchanov, D., Ashukha, A., and Vetrov, D. P. (2017), “Structured Bayesian Pruning via Log-Normal Multiplicative Noise,” in Proceedings of the 30th Advances in Neural Information Processing Systems (NIPS 2017), pp. 6775–6784, Long Beach, CA, USA.
- Paszke, A., Gross, S., Massa, F., Lerer, A., Bradbury, J., Chanan, G., Killeen, T., Lin, Z., Gimelshein, N., Antiga, L., Desmaison, A., Kopf, A., Yang, E., DeVito, Z., Raison, M., Tejani, A., Chilamkurthy, S., Steiner, B., Fang, L., Bai, J., and Chintala, S. (2019), “PyTorch: An Imperative Style, High-Performance Deep Learning Library,” in Advances in Neural Information Processing Systems 32, pp. 8024–8035, Curran Associates, Inc.
- Pati, D., Bhattacharya, A., and Yang, Y. (2018), “On Statistical Optimality of Variational Bayes,” in Proceedings of the Twenty-First International Conference on Artificial Intelligence and Statistics, eds. A. Storkey and F. Perez-Cruz, vol. 84 of Proceedings of Machine Learning Research, pp. 1579–1588, PMLR.
- Pollard, D. (1991), “Bracketing methods in statistics and econometrics,” in Nonparametric and semiparametric methods in econometrics and statistics: Proceedings of the Fifth International Symposium in Econometric Theory and Econometrics, eds. W. A. Barnett, J. Powell, and G. E. Tauchen, pp. 337–355, Cambridge, UK: Cambridge University Press.
- Polson, N. and Ročková, V. (2018), “Posterior Concentration for Sparse Deep Learning,” in 32nd Conference on Advances in Neural Information Processing Systems (NeurIPS 2018), pp. 930–941, Montréal, Canada.
- Ramachandran, P., Zoph, B., and Le, Q. V. (2017), “Searching for Activation Functions,” CoRR, abs/1710.05941.
- Scardapane, S., Comminiello, D., Hussain, A., and Uncini, A. (2017), “Group sparse regularization for deep neural networks,” Neurocomputing, 241, 81–89.
- Schmidt-Hieber, J. (2020), “Nonparametric regression using deep neural networks with ReLU activation function,” The Annals of Statistics, 48, 1875–1897.
- Sun, Y., Song, Q., and Liang, F. (2021), “Consistent Sparse Deep Learning: Theory and Computation,” Journal of the American Statistical Association, 0, 1–42.
- Wen, W., Wu, C., Wang, Y., Chen, Y., and Li, H. (2016), “Learning Structured Sparsity in Deep Neural Networks,” in Proceedings of the 29th Advances in Neural Information Processing Systems (NIPS 2016), Barcelona, Spain.

Zhang, C., Bengio, S., Hardt, M., Recht, B., and Vinyals, O. (2017), “Understanding deep learning requires rethinking generalization,” in 5th International Conference on Learning Representations (ICLR 2017), Toulon, France.

Zhu, M. and Gupta, S. (2018), “To Prune, or Not to Prune: Exploring the Efficacy of Pruning for Model Compression,” in 6th International Conference on Learning Representations (ICLR 2018), Workshop Track Proceedings, Vancouver, Canada.